



DOCTORAL THESIS NO. 2024:5
FACULTY OF NATURAL RESOURCES AND AGRICULTURAL SCIENCES

Greenhouse gas fluxes from drained peatland

Measurement techniques and management impacts

HANNES KECK

Greenhouse gas fluxes from drained peatland

Measurement techniques and management impacts

Hannes Keck

Faculty of Natural Resources and Agricultural Sciences

Department of Ecology

Uppsala



SWEDISH UNIVERSITY
OF AGRICULTURAL
SCIENCES

DOCTORAL THESIS

Uppsala 2024

Acta Universitatis Agriculturae Sueciae
2024:5

ISSN 1652-6880

ISBN (print version) 9978-91-8046-274-7

ISBN (electronic version) 978-91-8046-275-4

<https://doi.org/10.54612/a.4h68t79f4i>

© 2024 Hannes Keck, <https://orcid.org/0000-0001-7592-2833>

Swedish University of Agricultural Sciences, Department of Ecology, Uppsala, Sweden

The summary chapter of this thesis is licensed under CC BY NC 4.0. To view a copy of this license, visit <https://creativecommons.org/licenses/by-nc/4.0/>. Other licences or copyright may apply to illustrations and attached articles.

Print: SLU Grafisk service, Uppsala 2024

Greenhouse gas fluxes from drained peatland. Measurement techniques and management impacts

Abstract

Agricultural use of drained peatlands has significant implications for national greenhouse gas (GHG) emission inventories. Once drained, peatlands emit large amounts of carbon dioxide (CO₂), may become small methane (CH₄) sinks and, with nitrogen fertilisation, may emit large quantities of nitrous oxide (N₂O). Studies on the influence of set-aside cropland in reducing GHG emissions from peatlands are rare, measurement techniques for continuous long-term observations are costly and detection of small fluxes is critical. This thesis investigated management effects on GHG fluxes from a cropland (CL) and an adjacent set-aside (SA) grassland on peat. An affordable relaxed eddy accumulation (REA) system for measuring continuous fluxes of CO₂, N₂O, CH₄, and water vapour (H₂O) was designed and tested. A convenient method for optimising chamber flux measurement duration and number of concentrations was developed and tested against experimental data. The SA site showed higher annual CO₂ emissions than the CL site (0.41 and 0.16 kg CO₂ m⁻² yr⁻¹, respectively). Nitrous oxide and CH₄ emissions had a minor influence on the climate effect at both sites. The REA system reliably measured GHG fluxes over complete growing seasons, based on a comparison of CO₂ and H₂O fluxes with an eddy covariance system. The chamber optimisation method yielded similar results to experimental data, and can be valuable in the planning phase of measurement campaigns. In conclusion, this thesis found no evidence that setting-aside agricultural land on peat reduced GHG emissions and emphasises the importance of affordable and reliable measuring equipment.

Keywords: Carbon dioxide, Methane, Nitrous oxide, Setting-aside farmland, Land sparing, Relaxed eddy accumulation, Eddy covariance, Detection limit.

Greenhouse gas fluxes from drained peatland. Measurement techniques and management impacts

Abstract

Jordbrukets användning av utdikade torvmarker har betydande konsekvenser för nationella inventeringar av utsläpp av växthusgaser. Utdikade torvmarker släpper ut stora mängder koldioxid (CO_2), blir till små metansänkor (CH_4), och kan släppa ut stora mängder lustgas (N_2O) vid användning av kvävegödsling. Studier om hur avsättningar av odlingsmark påverkar växthusgasutsläppen från torvmarker är sällsynta, och mättekniker för kontinuerliga, långsiktiga observationer är kostsamma. Dessutom är förmågan till detektion av små flöden kritisk. I denna avhandling undersöktes effekten av jordbruksmetoder på växthusgasflöden från två intilliggande torvmarker, en odlingsmark (CL) och en gräsmark som tagits ur bruk (SA). Dessutom utformades och testades ett kostnadseffektivt eddy ackumuleringssystem med lättade krav (Relaxed Eddy Accumulation; REA) för att mäta kontinuerliga flöden av CO_2 , N_2O , CH_4 och vattenånga (H_2O). En praktisk metod för att optimera varaktigheten och antalet koncentrationer för flödesmätning i en kammare utvecklades även, och jämfördes med experimentella data. SA-marken visade högre årliga CO_2 -utsläpp än CL-platsen (0,41 respektive 0,16 $\text{kg CO}_2 \text{ m}^{-2} \text{ år}^{-1}$). Utsläppen av N_2O och CH_4 påverkade klimateffekten på båda platserna till en mindre grad. REA-systemet mätte på ett tillförlitligt sätt växthusgasflöden över hela växtsäsonger, vilket en jämförelse av CO_2 - och H_2O -flöden med ett eddy kovarianssystem visade. Metoden för kammaroptimering gav resultat som överensstämmer med experimentella data och kan vara ett värdefullt verktyg för planeringsfasen av mätningar. Sammanfattningsvis fann denna avhandling inga bevis på att avsättning av jordbruksmark på torv leder till en minskning av växthusgasutsläpp, och betonar vikten av prisvärd och tillförlitlig mätutrustning..

Nyckelord: Koldioxid, Metan, Lustgas, Avsättning av jordbruksmark, Markanvändning, Relaxed eddy accumulation, Eddy covariance, Detektionsgräns.

Dedication

To all fellow procrastinators, you can do it. Tomorrow.

Contents

List of publications.....	11
Scientific contributions outside the scope of this thesis	13
List of tables	15
List of figures	17
Abbreviations and symbols	21
1. Introduction.....	25
1.1 Background.....	25
1.1.1 Peatlands.....	25
1.1.2 The value of peatlands	25
1.1.3 Biogeochemistry of peatlands.....	26
1.2 Measurement techniques.....	30
1.2.1 Chamber technique	30
1.2.2 Eddy covariance	31
1.2.3 Relaxed Eddy Accumulation.....	32
1.2.4 System comparison	34
2. Objectives.....	37
3. Methods	39
3.1 Site description	39
3.2 Paper I	41
3.3 Paper II	44
3.4 Paper III	46
4. Results.....	49
4.1 Paper I	49
4.1.1 Comparison of CO ₂ fluxes measured by REA and EC...	49
4.2 Paper II	51

4.2.1	Influence of measurement duration on flux estimate precision.....	52
4.2.2	Influence of number of concentration measurements on flux estimate precision	55
4.3	Paper III	56
5.	Discussion	61
5.1	Paper I	61
5.2	Paper II	62
5.3	Paper III	64
6.	Conclusions and future perspectives.....	67
	References	69
	Popular science summary	77
	Populärvetenskaplig sammanfattning	79
	Populärwissenschaftliche Zusammenfassung	81
	Acknowledgements	83

List of publications

This thesis is based on the work contained in the following papers, referred to by Roman numerals in the text:

- I. Grelle A., Keck H. (2021). Affordable relaxed eddy accumulation system to measure fluxes of H₂O, CO₂, CH₄ and N₂O from ecosystems. *Agricultural and Forest Meteorology*, 307, 108514. <https://doi.org/10.1016/j.agrformet.2021.108514>
- II. Keck H., Meurer K., Fiedler J., Grelle A., Jordan S. (Submitted). Optimisation of sampling strategy for greenhouse gas flux estimations using non-steady-state chambers and fast analysers.
- III. Keck H., Meurer K.H.E., Jordan S., Kätterer T., Hadden D., Grelle A. (Submitted). Agricultural soil management of a drained peatland affecting CO₂, N₂O, and CH₄ fluxes in central Sweden.

Paper I is reproduced with the permission of the publisher.

The contribution of Hannes Keck to the papers included in this thesis was as follows:

- I. Co-author. Contributed to: REA system design, fieldwork, maintenance, data analysis, and writing of the manuscript.
- II. Main author. Conceived the initial idea, planned the experimental work together with the second and last author. Conducted the experimental work, data processing, analysis, and modelling. Wrote the manuscript with assistance from the co-authors.
- III. Main author. Conducted the fieldwork together with the fifth and last author. Processed and analysed the data with the assistance of the last author. Wrote the manuscript with the assistance of the co-authors.

Scientific contributions outside the scope of this thesis

Keck H., Strobel B.W., Gustafsson J.P., Koestel J. (2017). Quantitative imaging of the 3-D distribution of cation adsorption sites in undisturbed soil. *SOIL*, 3, 177-189. <https://doi.org/10.5194/soil-3-177-2017>

Callesen I., Keck H., Andersen T.J. (2018). Particle size distribution in soils and marine sediments by laser diffraction using Malvern Mastersizer 2000 - method uncertainty including the effect of hydrogen peroxide pretreatment. *Journal of Soils and Sediments*, 18, 2500-2510. <https://doi.org/10.1007/s11368-018-1965-8>

Felde V.J.M.N., Rodriguez-Caballero E., Chamizo S., Rossi F., Uteau D., Peth S., Keck H., De Philippis R., Belnap J., Eldridge D.J. (2020). Comment on 'Kidron, G. J. (2018). Biocrust research: A critical view on eight common hydrological-related paradigms and dubious theses. *Ecohydrology*, e2061'. *Ecohydrology*, 13, e2215. <https://doi.org/10.1002/eco.2215>

Rychel, K., Koestel, J., Keck, H., Meurer, K.H.E., Kätterer, T. (Manuscript). Greenhouse gas emissions as affected by N fertiliser placement depth and soil structure under controlled conditions.

List of tables

Table 1. *Annual and summer (May to August) rainfall and mean annual and summer temperature in the study region. Precipitation data were retrieved from the Swedish Meteorological and Hydrological Institute. Source: SMHI (2023); adapted from Paper III.* 41

Table 2. *Mean greenhouse gas (GHG) fluxes (carbon dioxide (CO₂), nitrous oxide (N₂O), and methane (CH₄)) during the summer months (May to August) 2018 to 2020 at the cultivated cropland site (CL) and set-aside grassland (SA), measured with transparent and opaque chambers, and on bare peat. Standard deviations (σ) and number of observations (n) are shown in brackets. GHG balance expressed in CO₂EQ. Source: adapted from Paper III.* 59

List of figures

- Figure 1.* Graphical representation of relevant nitrogen (N) and carbon (C) cycling processes in (left) drained and (right) natural peatland. The processes within the grey-shaded area are sensitive to oxygen concentrations, but can occur simultaneously within drained or natural peatland. DOC: dissolved organic C, DNRA: dissimilatory nitrate reduction to ammonium, ANAMMOX: anaerobic ammonium oxidation..... 28
- Figure 2.* Schematic diagram of (left) the eddy covariance method and (right) the relaxed eddy accumulation method..... 33
- Figure 3.* Location of the cultivated (CL) site and the set-aside (SA) grassland site in central Sweden. Source of satellite image: Eniro.se (2023)..... 40
- Figure 4.* Diagram illustrating the working principles of the relaxed eddy accumulation (REA) system. C1 to C6 represent the control ports of the SDM-CD16AC relay controller. Source Paper I. 42
- Figure 5.* Detection limit (DL) of the relaxed eddy accumulation system for nitrous oxide (N₂O), methane (CH₄), carbon dioxide (CO₂), and water vapour (H₂O) fluxes. Source: adapted from Paper I..... 43
- Figure 6.* Relationship between measurement duration [s], number of concentration measurements per gas flux estimate and rate of change (R_c [ppbv s⁻¹]) in gas concentration at analyser precision of p = 4 ppbv. Source: Paper II. 46

Figure 7. Carbon dioxide (CO₂) fluxes measured by eddy covariance (EC, blue line), relaxed eddy accumulation (REA, red line), and transparent chambers (black dots with bars indicating standard deviation) during September 2018. Source: adapted from Paper I. 50

Figure 8. Water vapour (H₂O) fluxes measured by eddy covariance (EC, blue line) and relaxed eddy accumulation (REA, red line) during spring 2020. Source: adapted from Paper I. 50

Figure 9. Carbon dioxide (CO₂) fluxes measured by eddy accumulation (EC) and relaxed eddy accumulation (REA) during summer 2018, with the identity line in black. Colour gradient indicating friction velocity. Source: adapted from Paper I. 51

Figure 10. Box plots of the carbon dioxide (CO₂), nitrous oxide (N₂O), and methane (CH₄) fluxes measured with transparent (yellow) and opaque (purple) chambers during the growing season 2019. The black dots represent individual measurements below the 25th or above the 75th percentile. Source: Paper II. 52

Figure 11. Box plots showing (A) differences between flux estimates of all measurement durations and flux estimates of the full 400 seconds (6:40 min.) of chamber closure duration and (B) differences between flux estimates per number of concentration measurements (*i.e.* number of concentration measurements < 500) and the flux estimate of the full dataset (*i.e.* number of concentration measurements = 500). Zero indicates no deviation from the median flux estimate of the full data set. Scattered dots represent individual data points. Transparent chamber measurements shown in yellow, opaque measurements in purple. Source: Paper II. 54

Figure 12. Relative type 2 error occurrence for carbon dioxide (CO₂), nitrous oxide (N₂O), and methane (CH₄) fluxes in transparent and opaque chamber measurements. (A) measurement duration and (B) number of concentration measurements per flux. Source: Paper II. 56

Figure 13. Mean daily precipitation and temperature (top panel) and mean daily carbon dioxide (CO₂) flux as net ecosystem exchange (NEE, dark grey), ecosystem respiration (R_{ECO}, black), gross primary production (GPP, light

grey), and cumulative NEE flux (Cum. NEE) at the cultivated cropland (CL, centre panel) and set-aside grassland (SA, lower panel) during the study period 2013 to 2019. Source: adapted from Paper III. 57

Figure 14. Comparison of the net ecosystem exchange (NEE) fluxes measured by eddy covariance (EC) and by transparent manual chambers at the cultivated cropland site (CL, blue triangles) and set-aside grassland site (SA, red dots). Solid line: $x=y$. Source: adapted from Paper III. 60

Abbreviations and symbols

ANAMMOX	Anaerobic ammonium oxidation
c	Dry mole fraction of an atmospheric tracer
C	Carbon
CO ₂ _HARV/HERB	Carbon losses due to harvest and herbivory
CH ₄	Methane
CL	Cultivated
CO ₂	Carbon dioxide
CO ₂ EQ	CO ₂ equivalent
Cum. NEE	Cumulative net ecosystem exchange of carbon dioxide
DL	Detection limit
DNRA	Dissimilatory nitrate reduction to ammonium
DOC	Dissolved organic carbon
d, e, f, k	Model parameters
F_{EC}	Turbulent flux measured by eddy covariance
F_{REA}	Turbulent flux measured by relaxed eddy accumulation
EC	Eddy covariance
EU	European Union
g	Gram
GHG	Greenhouse gas

GPP	Gross primary production
GWP ₁₀₀	Global warming potential based on 100 years
H ₂ O	Water (vapour)
H_{eff}	Effective chamber height
Hz	Hertz
K	Kelvin
L	Litre
m	Metre
M	Molar mass
MDS	Marginal distribution sampling
MEF	Minimum expected flux
mol	Mole
n	Number of observations
N	Nitrogen
N ₂ O	Nitrous oxide
NEE	Net ecosystem exchange of CO ₂
NO	Nitric oxide
NO ₂ ⁻	Nitrite
NO ₃ ⁻	Nitrate
O ₂	Atmospheric oxygen
p	Precision
P	Pressure
Pa	Pascal
ppbv	Parts per billion by volume
ppmv	Parts per million by volume
Pg	Petagrams; 10 ¹⁵ g

PTFE	Polytetrafluoroethylene
R	Ideal gas constant
R_C	Rate of change
REA	Relaxed eddy accumulation
R_{ECO}	Ecosystem respiration
R_{SOIL}	Soil respiration
s	Second
SA	Set-aside
T	Temperature
ustar	Friction velocity
v.	Version
V DC	Volt direct current
w	Vertical wind speed
w_0	Dead-band
yr	Year
3D	Three-dimensional
β	A coefficient
ρ	Air density
σ	Standard deviation
σ_w	Standard deviation of vertical wind speed
°C	Degrees Celsius

1. Introduction

1.1 Background

1.1.1 Peatlands

Peatlands cover about 3% of the global terrestrial surface (Xu et al., 2018) and store around 598 Pg carbon (C), which represents about 21% of the global soil organic C stock estimated to 2800 Pg C (Leifeld and Menichetti, 2018; Jackson et al, 2017). Around 13% of the world's peatlands have been drained for agriculture, forestry or peat extraction (Saurich et al., 2021), turning peatlands from C sinks or near C neutrality into major C sources. Under current circumstances, *i.e.* with no additional drainage, drained peatlands emit about 1.9 Pg carbon dioxide (CO₂) equivalents (CO_{2EQ}) per year globally (Leifeld and Menichetti, 2018). This represents about 4.7% of global anthropogenic greenhouse gas (GHG) emissions, *i.e.* more than the annual contribution from global civil aviation (Ritchie, 2020).

Peat is formed by incompletely degraded organic material accumulating over millennia under water saturation or a cool climate. According to the World Reference Base for Soil Resources (WRB), a peat soil is categorised as a histosol with a peat layer of at least 10 cm thickness at the surface, overlaying lithic or paralithic material, or a peat layer of at least 40 cm thickness that starts within the top 30 cm of the soil profile (WRB, 2015). Peatlands are ecosystems in which the soil is dominated by peat (IPCC, 2022).

1.1.2 The value of peatlands

Undisturbed peatlands provide many ecosystem services. As large C sinks and C stores they contribute to global climate regulation and exert a net

cooling effect on the planet (Bonn et al., 2016; Frolking and Roulet, 2007; Yu et al., 2011). They can also regulate local climate due to their shallow water table and can affect natural humidity by higher latent heat fluxes compared with their surroundings (Helbig et al., 2020), or by their higher albedo compared with, *e.g.* a neighbouring peat extraction site or a bare agricultural peat soil (Worrall et al., 2019). Furthermore, intact peatlands influence local hydrology, *e.g.* they can act as a filter by removing excess nutrients from groundwater or regulating local groundwater recharge or discharge (Bonn et al., 2016). They represent biodiversity hot spots with many rare plant and bird species depending on the unique habitat they support, and provide recreational and tourism opportunities (Bonn et al., 2016). Most of these services are “hidden” in the sense that they are not easily monetised. However, the soil-forming process of peatlands represents an ecosystem service that can be economically exploited. Peat extraction, forestry and agriculture on drained peatlands are examples of how drained peatlands are used. However, such use is unsustainable in the sense that the peat is degraded or even completely removed and, consequently, most other ecosystem services lose their functions. Through peatland drainage, local hydrology is changed significantly, jeopardising the functions of a peatland as a hydrological buffer and filter (Holden et al., 2004). In addition, local biodiversity may decrease as a result of drainage and the peat will degrade much faster when subjected to higher oxygen (O₂) levels, often transforming from a CO₂ sink into a CO₂ source (Evans et al., 2021; Holden et al., 2004; Joosten and Clarke, 2002). Peat extraction destroys the natural ecosystem because the peat itself is partially or completely removed (Joosten and Clarke, 2002).

1.1.3 Biogeochemistry of peatlands

Peat formation depends on the prevailing aeration level, defined mainly by local hydraulic conditions and by the living plants, often bryophytes, reeds, and other adapted organisms, that thrive within a very wet but still aerated top layer (the acrotelm). The acrotelm is formed by constant accumulation of dead plant material. Inside this layer, organic material is still subject to decomposition, but as more organic material is added to the surface, lower layers will gradually submerge into a water-logged, anaerobic zone (the catotelm), where no significant decomposition takes place. Through this

process, boreal peatlands accumulated an estimated 427 Pg C during the postglacial period (Leifeld and Menichetti, 2018).

Most undisturbed peatlands act as sinks of CO₂, are sources of methane (CH₄) and can emit small amounts of nitrous oxide (N₂O) (Frolking and Roulet, 2007; Leppelt et al., 2014). Inside the anaerobic environment of the catotelm, at low redox potential, microorganisms (methanogens) are able to use organic material instead of O₂ as electron acceptors to fuel their metabolism. Thus, they reduce organic material and CH₄ is formed (Bräuer et al., 2020). This CH₄ is transported via ebullition and diffuses through the peat matrix to the soil surface and is emitted from the ecosystem. Under anaerobic conditions, nitrogen (N) in different oxidation states can act as an electron acceptor instead of O₂, so NO₃⁻, NO₂⁻, NO, and N₂O are thermodynamically favourable compared with organic C. Nitrogen is reduced via microbial pathways such as denitrification, nitrifier-denitrification, dissimilatory nitrate reduction to ammonium, and anaerobic ammonium oxidation, or by abiotic pathways such as chemical decomposition of hydroxylamine and chemodenitrification (Butterbach-Bahl et al., 2013) (Figure 1). During these processes, N₂O can be formed as an intermittent or end product and diffuses to the peat surface to be emitted from the ecosystem. Due to low N availability in most natural peatlands, the N₂O emissions are low (Leppelt et al., 2014).

Around 17% of European peatlands have been drained for agricultural use as croplands or grasslands (Christensen et al., 2004; Evans et al., 2021). Once drained, the biogeochemistry of peatlands changes dramatically (Figure 1). This is predominantly due to a change in hydrological status and its effect on O₂ diffusivity and availability. Lack of water in the peat matrix increases O₂ diffusion 10⁴ fold and microorganisms can switch from less thermodynamically favourable electron acceptors to O₂. This drastically increases the decomposition of organic material, and thus the production of CO₂. If agriculture is practised, activities such as tillage can lead to a temporal increase in available O₂ and further increase CO₂ production from peatlands. Drainage turns peatlands from CO₂ sinks to CO₂ sources, but at the same time the higher O₂ availability within the peat layers often results in increasing activity of methanotrophic microorganisms that use CH₄ as an energy source for their metabolism (Lai, 2009). This turns peatlands into net CH₄ sinks. Overall, drainage of peatlands results in an increase in C emissions expressed as CO₂EQ (Evans et al., 2021). For peatlands to be used

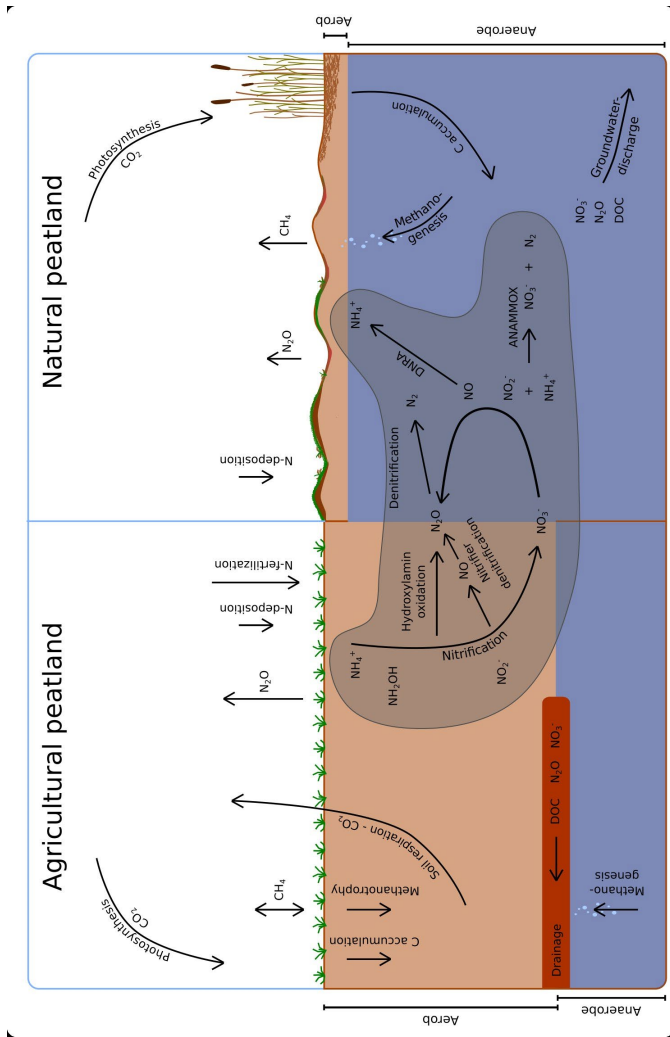


Figure 1. Graphical representation of relevant nitrogen (N) and carbon (C) cycling processes in (left) drained and (right) natural peatland. The processes within the grey-shaded area are sensitive to oxygen concentrations, but can occur simultaneously within drained or natural peatland. DOC: dissolved organic C, DNRA: dissimilatory nitrate reduction to ammonium, ANAMMOX: anaerobic ammonium oxidation.

productively for farming, N fertiliser usually needs to be applied. Therefore, N availability can be considerably higher on agricultural peatlands than on natural peatlands. Reactive N is not only used by plants, but also by microorganisms. Under anaerobic conditions, N in the form of NO_3^- or NO_2^- is used as an electron acceptor and, through a chain of reactions, is reduced to N_2O or elemental N. For N_2O formation to take place, the soil environment needs to be sufficiently reductive, as is usually the case under O_2 deprivation when soils or soil aggregates are wet and O_2 diffusion is limited. Depending on temperature and with sufficient available reactive N (e.g. NO_3^- or NO_2^-) and C, N_2O formation can take place. However, due to the dependence on environmental conditions and the complexities of microbial N_2O formation pathways, N_2O production can be very sporadic and spatially heterogeneous.

Around 3 to 5% of total peatland area in the Nordic countries is used for agriculture (Kløve et al., 2017), but this relatively small land area makes a major contribution to national GHG emissions. In Sweden, around 2% of the original peatland area (0.5% of total land area) is under agricultural use and is responsible for about 6 to 8% of national GHG emissions (Berglund and Berglund, 2010; Kløve et al., 2017). In Finland, 3% of total peatland is responsible for about 8% of national GHG emissions, while in Norway about 4% of total peatland contributes 3 to 4% of national GHG emissions (Grønlund et al., 2008; Kasimir-Klmedtsson et al., 1997; Kløve et al., 2017). To reduce the impact of farmland (including agricultural peatlands) on the environment and its contribution to climate change, setting-aside of agricultural land is a widely used approach within the European Union (EU). Under the EU Common Agricultural Policy, direct payments are provided to farmers for setting-aside of agricultural peatland as permanent grassland with no cultivation and no use of fertilisers or pesticides (EU Regulation No. 1307/2013, 2013). This may be effective in increasing local biodiversity and in reducing NO_3^- or pesticide leaching, but it seems an ineffective approach for protecting C stores in peat soil and reducing GHG emissions. Evans et al. (2021) found that effective water table depth within peatlands (reflecting the peat layer that is exposed to aerobic conditions) is the main factor controlling C emissions from peatlands. Supporting these findings, studies investigating the effects of different management intensities on local GHG budgets or comparing the GHG flux dynamics of set-aside farmland with those of active cropland have found that higher agricultural management intensity on Nordic

peatlands does not result in significantly higher GHG emissions (Berglund et al., 2021; Hadden and Grelle, 2017; Maljanen et al., 2010, 2007).

1.2 Measurement techniques

1.2.1 Chamber technique

The manual chamber technique is widely used for GHG flux monitoring because of its simplicity and low cost of equipment. It involves placing a chamber on the soil surface and determining the rate of change of the gas concentration inside the chamber's headspace air. Based on the rate of change, the gas flux between the soil and the atmosphere can be estimated. If no gas analyser is available in the field, air samples can be taken from the chamber's headspace by vial sampling and GHG concentrations can be analysed in the laboratory. It is also possible to measure the rate of change in the field by connecting a gas analyser directly, or via an air circulation system, to the chamber's headspace. In both cases, the chamber still needs to be placed on its base rings by manual means. In contrast, an automatic chamber system is capable of measuring GHG fluxes with high temporal frequency without the need for manual placement of the chambers, and thus has the advantage of reducing the labour input considerably and yielding continuous measurements.

Chamber measurements are particularly useful for treatment comparisons or for measurements on limited areas to investigate *e.g.* spatial flux heterogeneities. However, the average flux of a large area can be difficult to capture with a limited number of chambers. Further disadvantages are the disturbance caused by chamber measurements, both during base-ring placement and during each measurement, when photosynthesis can be disturbed and the diffusion gradient between soil and chamber headspace is altered.

To calculate the gas flux during a chamber measurement, a model needs to be fitted to describe the change in the gas concentration over time. In the literature, different models are commonly used. The simplest is a linear model (*e.g.* Lundegårdh, 1927), which requires the data to follow a linear trend, otherwise there is a risk of substantial flux under- or over-estimation (Kutzbach et al., 2007; Pedersen et al., 2010). As non-linear alternatives, other empirical methods such as exponential models or quadratic models can

be applied (Kutzbach et al., 2007; Wagner et al., 1997) to capture the non-linear trends typical of extended measurement periods. However, at small flux magnitudes, non-linear models exhibit higher uncertainty and thus lead to higher detection limit (DL) than linear models (Parkin et al., 2012). A physical-based non-linear model for estimating chamber gas fluxes was developed by Hutchinson and Mosier (1981). Since the change in headspace gas concentration during a chamber measurement influences the diffusion gradient from the soil into the chamber, linear models can often only describe the concentration change within the chamber over a short initial period. The length of this period depends mainly on the gas flux magnitude and the size of the chamber. If the gas concentration in the chamber headspace increases over time, the diffusion gradient decreases and so does the flux. Conversely, in transparent chambers during photosynthesis, the CO₂ concentration decreases over time, increasing the diffusion gradient from soil to chamber and thus increasing the flux. In a larger chamber with a larger internal volume or with lower flux magnitude, the change from an approximately linear to a non-linear rate of change occurs later in time than with a smaller chamber or higher flux. The decision on whether to use a linear or non-linear model can be made based on statistical comparisons of models or on visual inspection of the fit (Fuss et al., 2020; Hüppi et al., 2018). In some cases, a combination of models is recommended (Pedersen et al., 2010).

1.2.2 Eddy covariance

With the eddy covariance (EC) method, continuous GHG flux measurements over long periods are possible. By measuring the GHG concentration and the vertical wind speed simultaneously, the gas flux can be directly derived through their covariance. Within the atmospheric boundary layer, transport processes are dominated by turbulence, rather than diffusion. Eddies, the elements of the turbulent mixing process, vary over large spatiotemporal scales. High in the boundary layer profile, large eddies dominate. On descending, the effect of surface friction increases and eddy size becomes smaller and smaller until their kinetic energy dissipates to heat. Large eddies can be hundreds of metres in diameter and take several minutes to pass the measurement point of an instrument. Small eddies, with sizes of a few centimetres, pass the measurement point of an instrument in fractions of a second. Thus small eddies define the minimum measurement frequency of

the instrumentation used (typically 10 to 20 Hz), whereas large eddies define the averaging period for flux calculation (typically 30 minutes).

A turbulent flux (F_{EC}) can be described by the mean product of the vertical wind speed (w), the dry mole fraction of a tracer of interest (c), and air density (ρ):

$$F_{EC} = \overline{\rho w c} \quad (1)$$

Turbulent time series data can be decomposed into a mean part (\bar{x}) and a fluctuating part (x') over an averaging time period. Thus, it is assumed that the state of a fluid in turbulent motion can be described by the sum of its mean and fluctuating part at any instant in time:

$$x = \bar{x} + x' \quad (2)$$

This so-called Reynold decomposition can be applied to Equation 1, giving:

$$F_{EC} = \overline{(\bar{\rho} + \rho')(\bar{w} + w')(\bar{c} + c')} \quad (3)$$

Opening the brackets in Equation 3 gives:

$$F_{EC} = \overline{\bar{\rho} \bar{w} \bar{c} + \bar{\rho} \bar{w} c' + \bar{\rho} w' \bar{c} + \bar{\rho} w' c' + \rho' \bar{w} \bar{c} + \rho' \bar{w} c' + \rho' w' \bar{c} + \rho' w' c'} \quad (4)$$

Equation 4 can be simplified by removing the mean deviations of an average (which are zero) and by the assumptions that air density variations and divergence or convergence are negligible over a flat and homogeneous surface. This leads to Equation 5, which is commonly used to calculate turbulent fluxes of GHG:

$$F_{EC} = \overline{\rho w' c'} \quad (5)$$

1.2.3 Relaxed Eddy Accumulation

Relaxed eddy accumulation (REA) is closely related to the EC method (Figure 2). However, there is no need to use a fast response analyser to measure gas concentrations (Businger and Oncley, 1990). Instead of measuring the gas concentrations at 10 Hz, the measurement system samples air from upward and downward directed airflow (updrafts and downdrafts) in two reservoirs by opening and closing a pair of fast-switching valves. After an averaging period (typically 30 minutes), the gas concentrations within the sampled air are analysed. The high frequency aspect is not

burdened on the analyser, but performed by the fast-switching valves. Therefore, an advantage of the REA method is that slow-response gas analysers can be used. This is valuable, particularly when no fast-response analysers are available, when their DL is too high for small flux magnitudes, or when low power consumption is essential. Thus, REA has been used for a wide range of tracers, such as CO₂, N₂O, CH₄, mercury, isotopes, aerosols, volatile organic compounds, etc. (Beverland et al., 1996; Desjardins et al., 2010; Gaman et al., 2004; Haapanala et al., 2006; Hargreaves et al., 1996; Osterwalder et al., 2016; Pattey et al., 2007; Ren et al., 2011; Riederer et al., 2014). But not yet for measuring fluxes of CO₂, N₂O, CH₄, and water vapour (H₂O) simultaneously and over complete agricultural seasons.

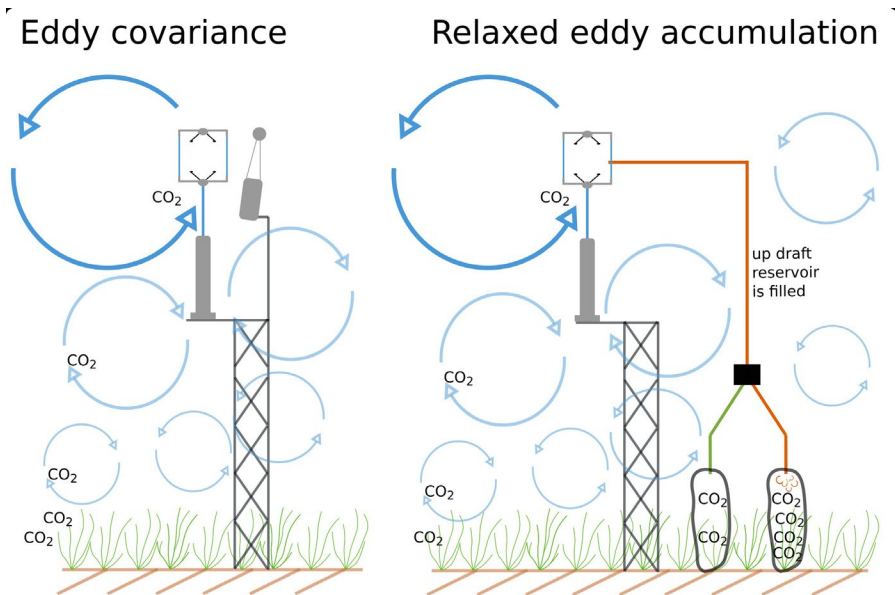


Figure 2. Schematic diagram of (left) the eddy covariance method and (right) the relaxed eddy accumulation method.

The mean flux over the sampling period is calculated as:

$$F_{REA} = \beta \sigma_w (C_{up} - C_{down}) \quad (6)$$

where σ_w is the standard deviation of the vertical wind speed, β is an empirical coefficient, and $C_{up} - C_{down}$ is the concentration difference between the updrafts and downdrafts. Coefficient β can be estimated as:

$$\beta = \frac{\overline{w'T'}}{\sigma_w(T_{up} - T_{down})} \quad (7)$$

where $\overline{w'T'}$ is the covariance between vertical wind velocity and air temperature measured with the EC method and $\sigma_w(T_{up} - T_{down})$ is the temperature difference between the sampled updrafts and downdrafts calculated by the REA approach.

For the REA system to provide reasonable flux estimates, it is important that the two reservoirs are filled with updraft or downdraft air only. This is challenging if the vertical wind speed is close to zero, because air may falsely be sampled as updraft or downdraft due to limited resolution and accuracy of the sonic anemometer. Thus, a threshold needs to be applied (dead-band, w_0). Within the limits of the dead-band no sampling takes place. A dynamic dead-band that scales with σ_w ensures that erroneous air sampling is avoided, that the sampling is adapted to turbulence conditions and therefore that air is continuously sampled both during day-time and night-time conditions.

1.2.4 System comparison

Each of the available methods has its merits and drawbacks. The chamber method is well suited for plot-scale GHG flux monitoring when treatment effects are of interest. It is also a valuable complement to the EC method if the latter does not measure all relevant GHGs due to technical or financial constraints. However, measurements with manual chambers are labour-intensive and capture only a snapshot in space and time. By using an automatic chamber set-up that is able to take regular measurements without supervision, these constraints can be avoided to some extent. However, even with an automatic system spatial limitations prevail. The EC method is capable of measuring continuous GHG fluxes over long periods and large areas, with little supervision needed. With a suitable set-up, fluxes of all relevant GHGs (CO_2 , N_2O , CH_4 , and H_2O) can be measured and, in contrast to the chamber method, the EC method measures them more directly, *i.e.* it does not rely on empirical constants. However, since source allocation is rather complex, treatment effects are difficult or impossible to capture. An EC system for measuring CO_2 , N_2O , CH_4 , and H_2O is expensive, relies on

several analysers and needs access to the power grid, due to high electricity demands. The REA method is capable of measuring all relevant GHGs with a single analyser and, due to its lower power consumption, can be run off-grid at remote locations. The installation costs are lower than those of a full EC system, but the maintenance needs are higher due to mechanical stresses on materials and valves in the REA system.

2. Objectives

In light of the fact that agricultural peatlands are large emitters of GHGs and considering the rapid pace of development of GHG flux monitoring systems, the objectives of this thesis were to:

- Construct an affordable, modular REA system for measuring continuous fluxes of CO₂, N₂O, CH₄, and H₂O from terrestrial ecosystems (Paper I)
- Evaluate and compare the performance of the REA system against an existing EC system sharing the same location and sonic anemometer (Paper I)
- Determine the influence of measurement duration and the number of concentration measurements per flux estimate on the uncertainty in flux estimates and the bias in individual chamber measurements (Paper II)
- Develop a simple and convenient method for calculating the minimum measurement duration or the minimum number of concentrations necessary for reliable N₂O or CH₄ flux measurements, while considering the precision of the analyser and the anticipated flux magnitude (Paper II)
- Quantify the GHG balance of two neighbouring sites on drained peat, a cultivated cropland and set-aside grassland (Paper III)
- Evaluate the effect of setting aside agricultural peatland on the GHG budget (Paper III)

3. Methods

3.1 Site description

Field measurements were carried out at two sites approximately 0.5 km apart on a drained peatland in central Sweden (Figure 3). Mean annual precipitation (1989 to 2019) is 590 mm yr⁻¹ and mean annual temperature is 5.9 °C (SMHI, 2023). For more details about the annual weather during the measurement period, see Table 1. Peat thickness at the cultivated (CL) site (60.0835° North, 17.233° East) is around 25 cm and that at the set-aside grassland (SA) site (60.079° North, 17.236° East) around 34 cm. The original peatland was drained in 1878 (Nerman, 1898). Before drainage and subsequent peat subsidence, the peat layer used to be much thicker than today. Estimated peatland-subsidence in Nordic countries is 0.5 to 2.5 cm yr⁻¹ (Berglund, 1996). For more than 10 years prior to the study, the CL site was used for cereal production. During the study period (2013 to 2019), the site was predominantly cultivated with spring wheat that was used as a sacrificial crop for wildlife and thus not harvested. Exceptions were the years 2016 and 2017. In 2016, no cultivation practices were performed and the following year, barley was grown and harvested (3.7 Mg ha⁻¹). In spring 2013 and 2014, the field was prepared using a mouldboard plough to a depth of 20 cm. In 2015 and 2017 to 2020, the soil was cultivated using a disc cultivator. Only in spring 2017 N fertiliser at a rate of 70 kg ha⁻¹ was applied.

For more than 30 years, the SA site was under permanent grassland. During this study, no management was carried out, except of an annual grass-cut in the years 2015 to 2019. All biomass was left in the field, except in 2018 when it was removed as hay.

At both sites, chemical soil properties at a depth of 5 to 15 cm were similar; with total C content of 33.6 and 31.7%, total N content of 2.03 and 1.93%, and C/N ratio of 16.5 and 16.4, for the CL and SA site, respectively (Berglund et al., 2021).

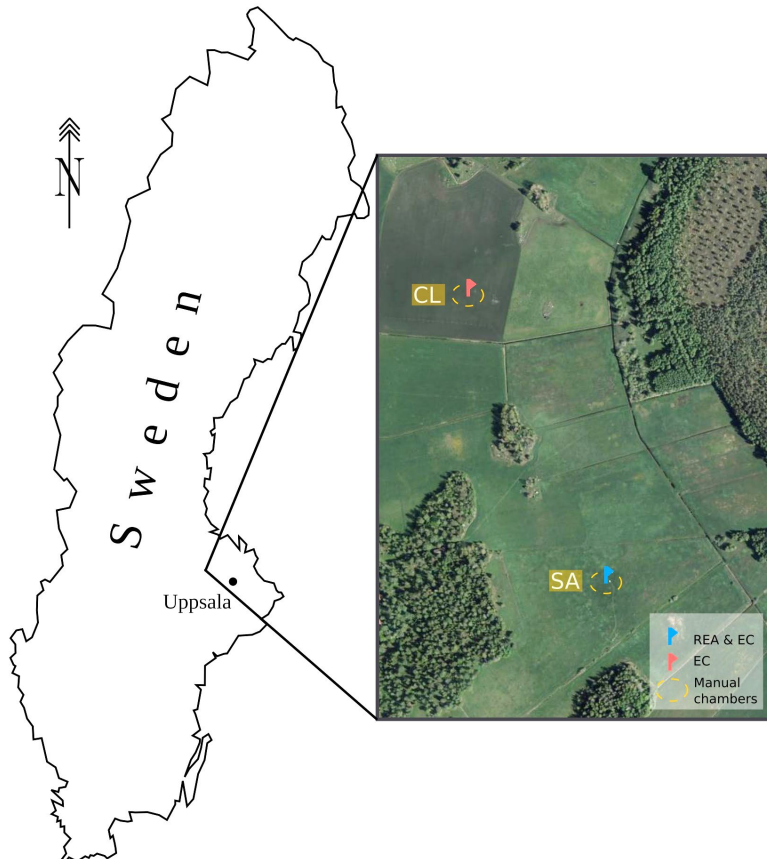


Figure 3. Location of the cultivated (CL) site and the set-aside (SA) grassland site in central Sweden. Source of satellite image: Eniro.se (2023).

Table 1. Annual and summer (May to August) rainfall and mean annual and summer temperature in the study region. Precipitation data were retrieved from the Swedish Meteorological and Hydrological Institute. Source: SMHI (2023); adapted from Paper III.

	Annual rainfall [mm]	Mean annual temperature [°C]	Summer rainfall [mm]	Mean summer temperature [°C]
2013	453	5.7	169	15.6
2014	521	7.4	179	15.4
2015	561	7.5	256	14.1
2016	488	7.1	206	15.5
2017	628	6.4	185	15.5
2018	495	7.8	151	18.0
2019	739	8.5	242	15.5

3.2 Paper I

The REA system was constructed with the following main components: a 3D ultrasonic anemometer (Solent 1012R3, Gill Instruments, Lymington, UK), two pairs of air reservoirs (12 L Tedlar bags, SKC 232-10, Eighty Four, PA, USA), a pair of fast-switching one-way stainless-steel solenoid valves (6011, Buerkert, Ingelfingen, Germany), a G2805 cavity ring-down spectrometer (Picarro Inc., Santa Clara, CA, USA), and a CR1000 Measurement and Control Datalogger and SDM-CD16AC relay driver (Campbell Scientific, Logan, UT, USA). The main principles of the REA system are shown in Figure 4.

The REA system was installed on the SA site, sharing the same sonic anemometer as an EC system that measured CO₂ and H₂O fluxes. The REA system sampled air from close to the sonic anemometer (about 15 cm away) for each updraft and downdraft separately into two air reservoirs by the action of the two fast-switching solenoid valves. By using separate sample lines for the updraft and downdraft air, no turbulent air-flow inside the lines was needed, and thus the flow rate was set to 0.8 L min⁻¹. To avoid

contamination, the airflow was maintained by vacuum boxes (IM2720, Pelican Products Inc., Torrance, CA, USA). These were evacuated or pressurised by air pumps (1420VDP Gardner Denver Thomas GmbH, Fürstentfeldbruck, Germany), depending on whether the air was sampled into the reservoirs or directed to the analyser. The necessary pressure difference between the interior of the vacuum boxes and the atmosphere was kept constant at -20 hPa for sampling and 20 hPa for evacuating. This was measured by 100KPDW differential pressure sensors (Fujikaru Ltd., Tokyo, Japan) and controlled by the CR1000 Data logger. The airflow towards the

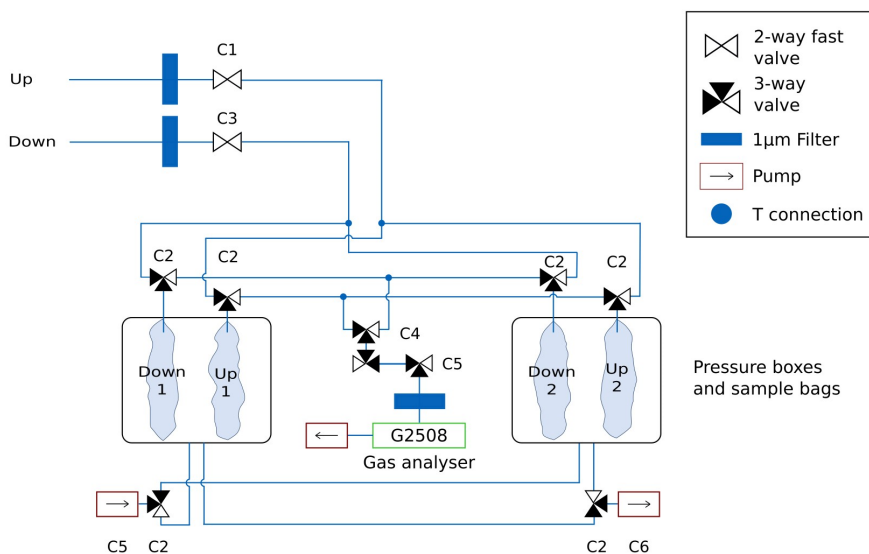


Figure 4. Diagram illustrating the working principles of the relaxed eddy accumulation (REA) system. C1 to C6 represent the control ports of the SDM-CD16AC relay controller. Source Paper I.

G2508 was facilitated by three-way stainless-steel solenoid valves (30334, Rotex, Maharashtra, India). With the exception of the G2508 analyser, all components are powered by 12 V DC. The whole system was built in a modular manner, so that it is easy to install and run at remote locations. By changing the analyser to a 12 V DC-powered device, it would even be possible to run it off-grid.

The G2508 analyser's standard deviations (σ) per gas species were determined by injection of a well-mixed standardised air sample (see Paper I). The σ values obtained were used to estimate the DLs of the REA system

for each gas species, by using Monte Carlo analysis. Zero-flux data were simulated 10^4 times, using the *rnorm* function in R (version 3.6.3; R Core Team, 2020) together with the mean gas concentration and the σ values of the analyser. Equation 6 was used to calculate the zero flux, with $\beta = 0.475$, the simulated data used as mean updraft and downdraft concentrations, and an ecosystem-typical σ_w ($0.063 < \sigma_w < 0.5$). As in Parkin et al. (2012), the DL was defined as the 97.5th-percentile. Obviously, this DL scales linearly with σ_w (see Figure 5) and therefore a value needs to be calculated for each value of σ_w .

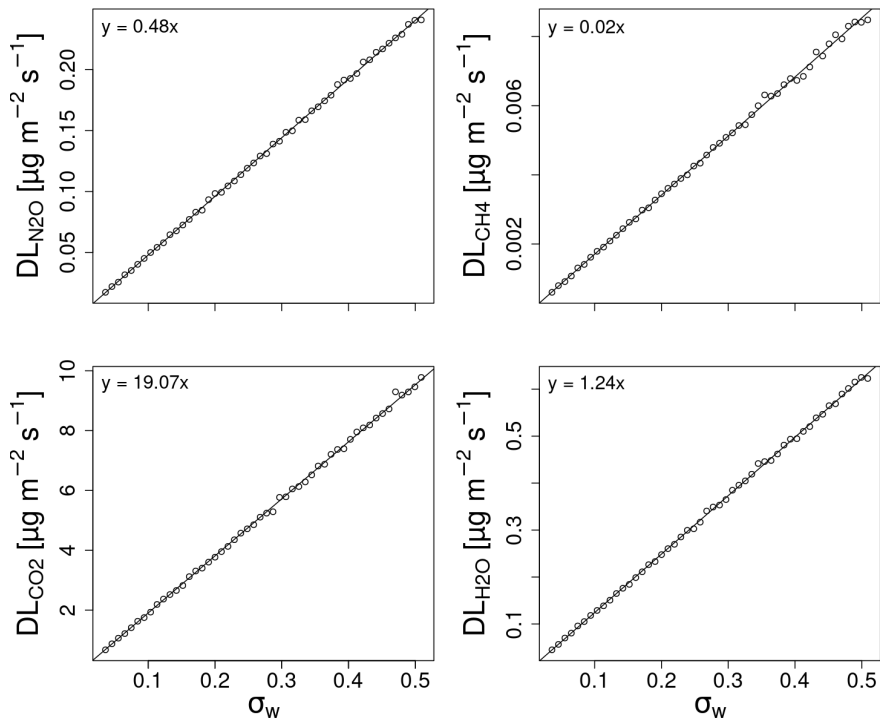


Figure 5. Detection limit (DL) of the relaxed eddy accumulation system for nitrous oxide (N_2O), methane (CH_4), carbon dioxide (CO_2), and water vapour (H_2O) fluxes. Source: adapted from Paper I.

3.3 Paper II

In paper II, chamber flux measurements were carried out at the SA site using a non-steady-state transparent chamber (volume: 0.01 m³; area: 0.028 m²). Transparent chamber measurements were used to estimate net ecosystem exchange (NEE) from the vegetation and soil within the chamber base rings. The same chamber was used, covered with a light-proof hood to conduct opaque measurements on the same base rings in order to estimate ecosystem respiration (R_{ECO}) or on bare peat to estimate soil respiration (R_{SOIL}). The chamber was connected via a custom-made air circulation system with the G2508 analyser, and the dry mole fractions of CO₂, N₂O, and CH₄ were reported approximately every second. Air circulation was ensured by 50 m polytetrafluoroethylene (PTFE) tubing (ScanTube, Helsingborg, Sweden; inner diameter 6 mm), an air pump, and a PTFE filter (1 µm, Merck Millipore, Darmstadt, Germany). Inside a flexible pipe, the PTFE tubing was installed together with a heating wire to avoid condensation. The flow rate was set to 1.3 L min⁻¹. After the chamber was installed on a base ring, 500 gas concentration measurements were taken over a period of 400 seconds and used for flux calculation. After each measurement, the air circulation system was flushed with ambient air for about two minutes or until stable gas concentrations were reached at atmospheric concentrations. The transparent and opaque measurements were conducted consecutively.

After retrieving the data from the G2508, they were treated so that (i) the measurement duration was reduced from 400 to 60 seconds in steps of 20 seconds (maintaining the same measurement frequency) and (ii) the measurement frequency (*i.e.* the concentration measurements per flux estimate) was reduced from 500 to 25 in steps of 25 and from 13 to 3 in single steps (maintaining the original measurement duration of 400 seconds).

With those reduced data sets, fluxes were calculated for each gas by quadratic regression using the *lm* function in the integrated development environment R studio (R version 4.2.3; R Core Team, 2023).

To develop a simple method for calculating minimum measurement duration and minimum number of concentration measurements per N₂O or CH₄ flux, values were simulated using a Monte Carlo approach to find the respective minimum detectable flux (Parkin et al., 2012). Data were generated to represent a zero flux, using random number generation (*rnorm* function in R). A range of gas analyser precisions values (N₂O: 0.001 ≤ *p* ≤ 500, CH₄: 0.001 ≤ *p* ≤ 500 ppbv) and atmospheric concentrations (339 ppbv

N₂O, 1.96 ppmv CH₄) were used as input variables. For each analyser precision value, measurement duration (60 to 1200 seconds), and number of concentrations (3 to 1400), 10³ zero-flux data sets were generated and the minimum detectable flux was defined as the 97.5th-percentile of the calculated flux (Parkin et al., 2012). This approach is computationally intensive, but allowed a three-dimensional surface model (Figure 6) to be fitted to each simulated data set using the python (v. 3.10) *curve_fit* function in the *scipy* module (Virtanen et al., 2020):

$$z = d x^e y^f \quad (8)$$

where z is the DL (in ppmv s⁻¹), x is the minimum number of concentration measurements per flux, y the minimum measurement duration (seconds), and d , e , and f are model parameters. The precision p (ppbv) of the analyser relates linearly to parameter d . With the median of the normal distributed parameters e ($\bar{e} = -0.407$) and f ($\bar{f} = 1.0014$) Equation 8 could be reformulated to:

$$MEF = k p x^{\bar{e}} y^{\bar{f}} \left(\frac{M P H_{eff}}{R T} \right) \quad (9)$$

where k is 0.0144 (ppbv s⁻²), H_{eff} is effective chamber height (m), M is molar mass (g mol⁻¹), P is pressure (kPa), R is ideal gas constant (L kPa K⁻¹ mol⁻¹), T is temperature (K), and MEF is minimum expected flux (mg m⁻² s⁻¹). Therefore, the minimum number of concentration measurements per flux (x) or the minimum measurement duration (y) for N₂O and CH₄ and a large range of gas analyser's precisions can be determined by using Equation 9.

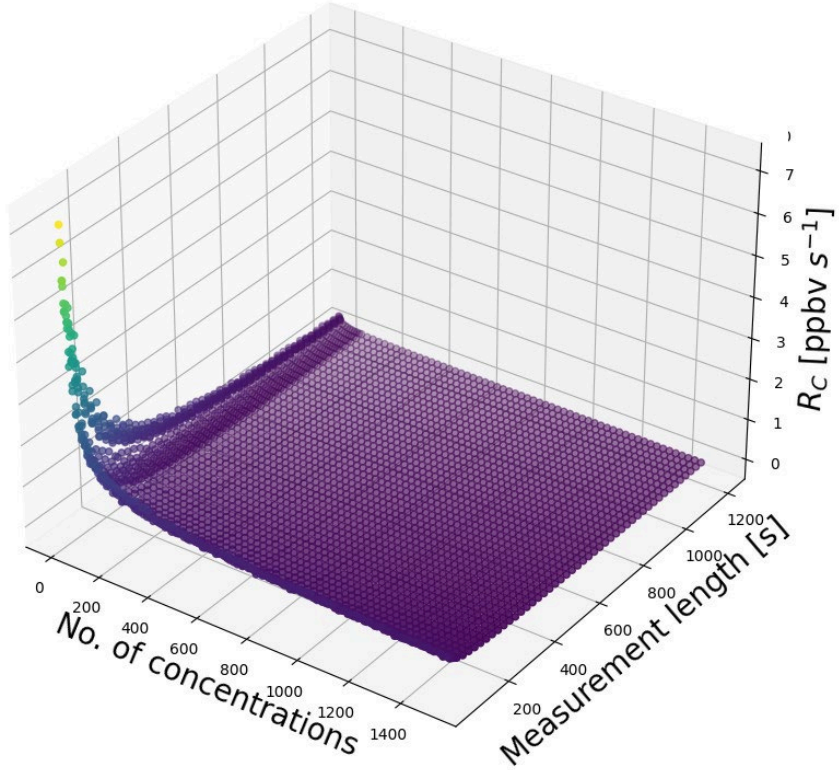


Figure 6. Relationship between measurement duration [s], number of concentration measurements per gas flux estimate and rate of change (R_c [ppbv s^{-1}]) in gas concentration at analyser precision of $p = 4$ ppbv. Source: Paper II.

3.4 Paper III

Eddy covariance measurements at the CL and SA sites began in autumn 2012. A closed path gas analyser (LI-6262, LI-COR inc., Lincoln Nebraska, USA) and a three-dimensional ultrasonic anemometer (Solent 1012R3, Gill Instruments, Lymington, UK) were installed at both sites. The air inlet was 2.5 m above the ground and sample air was transported at 12 L min^{-1} through a sample line (high-density polyethylene) with a diameter of 6 mm. At the SA site, during 2012 and 2014, a GGA-EP Off-Axis Integrated Cavity Output Spectroscopy analyser (Los Gatos Research Inc., San Jose, CA, USA) connected via a PTFE tube (10 mm diameter) to a dry scroll pump was

used instead of the LI-6262 gas analyser. In 2019, the LI-6262 was replaced with an open path analyser (LI-7500, LI-COR inc., Lincoln Nebraska, USA).

In the period 2018 to 2020, additional GHG flux measurements were taken at both sites by means of manual chambers. The transparent chamber included a thermometer, a vent tube, and a fan. During sampling, the chamber remained closed for 12 minutes and four vials were taken for subsequent determination of dry mole fraction of CO₂, CH₄, and N₂O by the Picarro G2508 gas analyser. On five base rings with intact vegetation, NEE was measured. By covering the same chamber with an opaque hood, ecosystem respiration (R_{ECO}) was measured on the base rings with vegetation and soil respiration (R_{SOIL}) on three base rings with no vegetation. At the SA site, NEE and R_{ECO} were measured on ten base rings and R_{SOIL} on five. However, a modified sampling method was chosen. The Picarro G2508 gas analyser was connected via an air circulation system to the chamber. For more details, consult the methods section of Paper II. No significant differences between the two sampling systems were found (Table S1 in Paper III). During each measurement, soil temperature readings at 5 cm depth next to the chamber and air temperature measurements in the chamber headspace air were taken. Additionally, a soil sample for the determination of gravimetric soil water content was taken adjacent to the chamber.

The raw EC data were processed using Ecoflux software (In Situ Flux Systems AB, Ockelbo, Sweden). A 30-minute block average was used and fluxes were calculated based on Aubinet et al. (1999), including lag determination by cross-correlation and two-fold coordinate rotation. Some data gaps occurred, mainly due to pump or power failures, representing 24.2 and 7.9% of the data over the whole measurement period for the CL and SA site, respectively. R studio (version 4.3.1; R Core Team, 2023) and the *ReddyProc* package (Wutzler et al., 2018) were used for further data processing. An *ustar* (friction velocity) filter was applied to exclude periods of stable atmospheric conditions (Papale et al., 2006). Outlier detection and removal was performed by the median absolute deviation method (Papale et al., 2006). Negative night-time fluxes were removed. The data gaps after post-processing amounted to 35.3 and 24.3% for the CL and SA site, respectively. Those gaps were filled using the marginal distribution sampling (MDS) method, which combines the look-up table and mean diurnal course method and decides on the most suitable method to use based upon availability of meteorological data for each gap (Reichstein et al., 2005). In

the rare event that a data gap could not be filled by the MDS method, the average value for the same date and time in all years was used to fill the gap. This approach needed to be applied to some periods in 2017 and 2018 for the CL site, when instrument failures were frequent.

4. Results

4.1 Paper I

4.1.1 Comparison of CO₂ fluxes measured by REA and EC

As the REA system was installed in parallel with an EC system, direct system comparison was possible. Both systems showed similar CO₂ and H₂O flux patterns and clear diurnal courses (Figure 7 and Figure 8). However, under stable atmospheric conditions (*i.e.* low *u*_{star} values), comparison of CO₂ flux measurements during the season of 2018 showed some deviation between the systems (Figure 9). Water vapour fluxes of both systems are in good agreement, occasionally low H₂O were reported by the REA system while the EC system measured larger fluxes, this discrepancy occurred predominantly during stable atmospheric conditions. Occasional negative H₂O fluxes were observed, likely originating from periods of dew formation (Figure 8).

Transparent chamber measurements aligned well with the observed CO₂ fluxes measured by both micrometeorological systems (Figure 7). A CO₂ budget comparison between the REA and EC systems based on non-gap-filled data yielded similar results during an extended period of sink activity from 22 June to 7 August 2018 (0.135 kg CO₂ m⁻² and 0.128 kg CO₂ m⁻² for the EC and REA system, respectively) (Paper I). A budget comparison of H₂O fluxes resulted in evapotranspiration of 21.6 and 19.0 mm for the EC and REA system, respectively (Paper I)

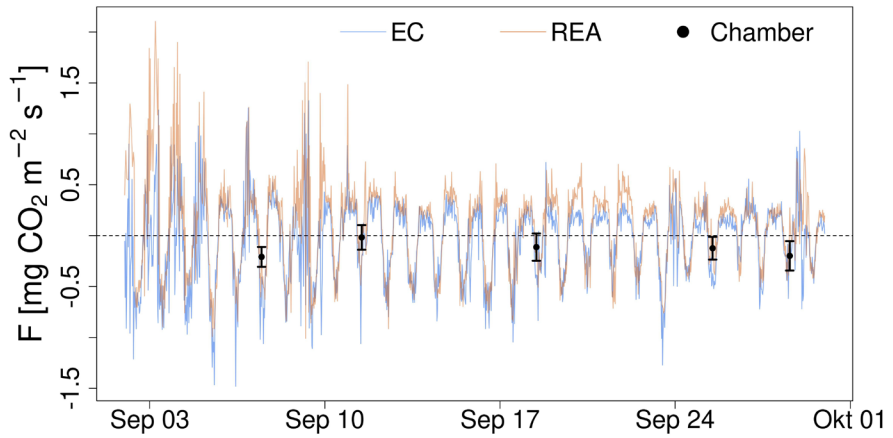


Figure 7. Carbon dioxide (CO_2) fluxes measured by eddy covariance (EC, blue line), relaxed eddy accumulation (REA, red line), and transparent chambers (black dots with bars indicating standard deviation) during September 2018. Source: adapted from Paper I.

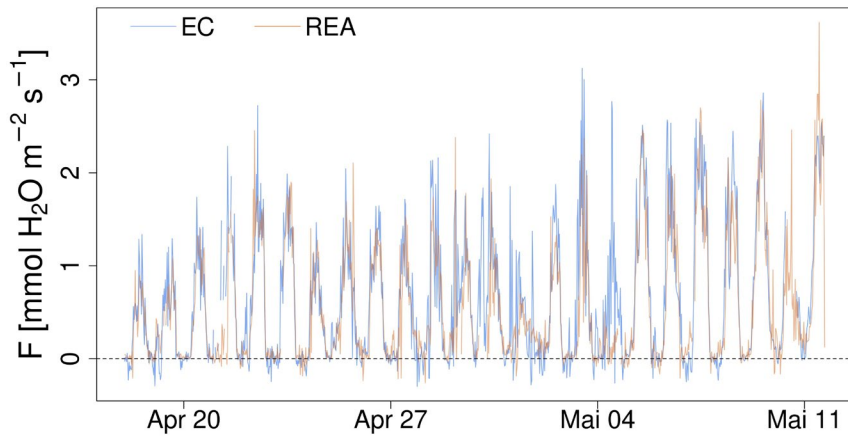


Figure 8. Water vapour (H_2O) fluxes measured by eddy covariance (EC, blue line) and relaxed eddy accumulation (REA, red line) during spring 2020. Source: adapted from Paper I.

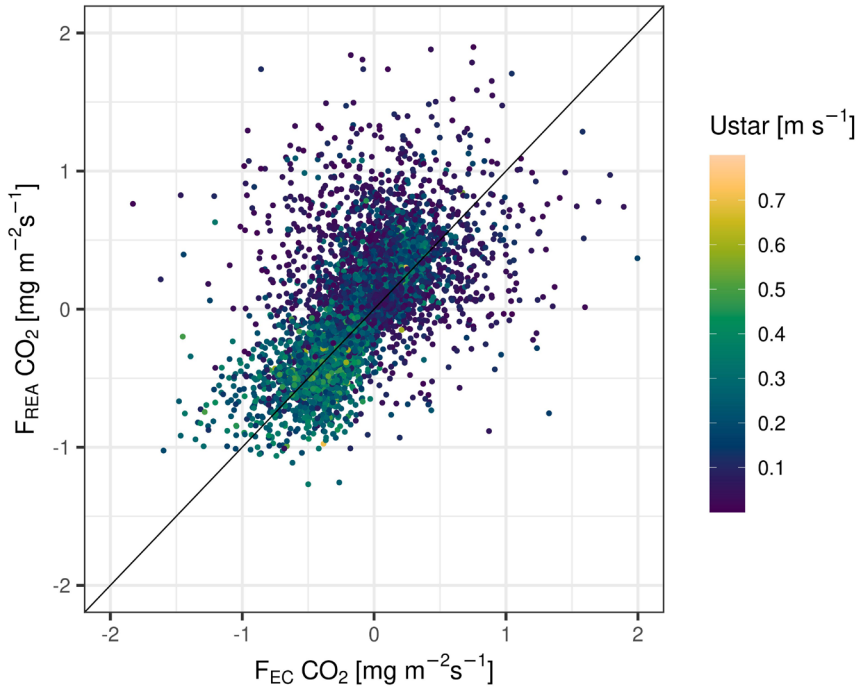


Figure 9. Carbon dioxide (CO₂) fluxes measured by eddy accumulation (EC) and relaxed eddy accumulation (REA) during summer 2018, with the identity line in black. Colour gradient indicating friction velocity. Source: adapted from Paper I.

4.2 Paper II

Fluxes of CO₂, N₂O, and CH₄ measured with transparent and opaque chambers are shown in Figure 10. As can be seen, CO₂ uptake in the transparent chambers due to photosynthesis and CO₂ release during opaque measurements due to respiration were distinctly different. Nitrous oxide fluxes were generally low and showed no difference between the transparent and the opaque chamber measurements. Methane uptake dominated during the measurement period and no difference between opaque and transparent measurements were found. The average flux measured by the transparent chamber was -313.2 , $6.0 \cdot 10^{-3}$ and $-0.014 \mu g m^{-2} s^{-1}$ and by the opaque chamber was 451.0 , $-1.5 \cdot 10^{-3}$ and $-0.015 \mu g m^{-2} s^{-1}$ for CO₂, N₂O, and CH₄ respectively. Detection limit in absolute terms for CO₂, CH₄, and N₂O was

0.31, $7.2 \cdot 10^{-3}$ and $5.8 \cdot 10^{-5}$ $\mu\text{g m}^{-2} \text{s}^{-1}$, respectively. Thus, 44% of N_2O fluxes were below the DL, whereas all CO_2 and CH_4 fluxes were above the DL.

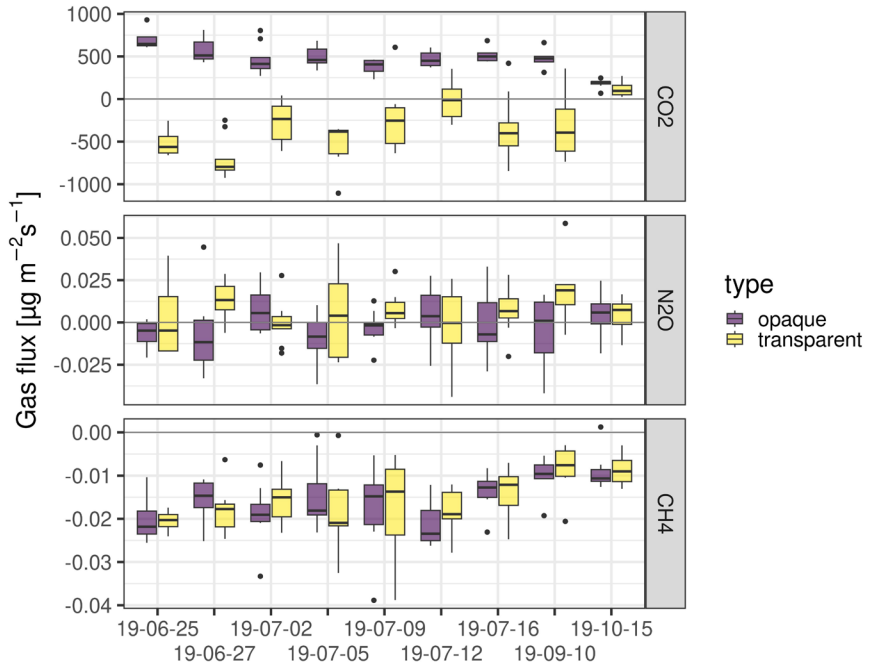


Figure 10. Box plots of the carbon dioxide (CO_2), nitrous oxide (N_2O), and methane (CH_4) fluxes measured with transparent (yellow) and opaque (purple) chambers during the growing season 2019. The black dots represent individual measurements below the 25th or above the 75th percentile. Source: Paper II.

4.2.1 Influence of measurement duration on flux estimate precision

The differences in flux estimates between the 400-second measurements and each shorter measurement duration are shown in Figure 11A. Shorter measurement duration caused greater variation, thus lowering the flux estimate precision for all three gases.

By determining the proportion of fluxes from the shortened data sets (measurement duration < 400 seconds) that exceeded the DL under the condition that the fluxes from the full data set (measurement duration = 400 seconds) were below the DL, type 1 error abundance (detecting a significant flux while the true flux is zero) was revealed. No evidence of type 1 errors were found for CO_2 or CH_4 fluxes of the shortened data at any measurement

duration between 60 and 400 seconds. Conversely, the proportion of fluxes from the shortened data sets that were below the DL under the condition that the respective fluxes from the full data set were above the DL revealed type 2 error abundance (detecting no significant flux while the true flux is not equal to zero). The CO₂ fluxes did not show any evidence of type 2 errors (Figure 12A). In transparent and opaque chamber measurements, the CH₄ fluxes exceeded type 2 error occurrence of 5% with a measurement duration of less than 80 seconds (Figure 12A). At measurement durations of less than 380 seconds, the type 1 and 2 error occurrence for N₂O flux estimates exceeded 5% for both opaque and transparent chambers (Figure 12A). This suggests that with the given flux magnitudes at the study site and the measurement system used, minimum measurement duration was approximately 380, 80, and 60 seconds for N₂O, CH₄, and CO₂, respectively.

Using Equation 9 with a minimum expected flux (MEF) of 0.009 $\mu\text{g m}^{-2} \text{s}^{-1}$ (using the 2.5th percentile of all fluxes that exceeded the DL) and concentration measurements at 1.25 Hz with analyser precision of $p = 3.8$ ppbv gave a minimum measurement duration for N₂O flux measurements of 330 seconds. With MEF for CH₄ of -0.0038 $\mu\text{g m}^{-2} \text{s}^{-1}$ (as defined above), the same concentration measurement frequency and $p = 0.37$ ppbv, the minimum measurement duration was 76 seconds. The minimum measurement duration estimated by the type 2 error occurrence and on Equation 9 corresponded well for CH₄ fluxes, but deviated by 50 seconds for N₂O fluxes.

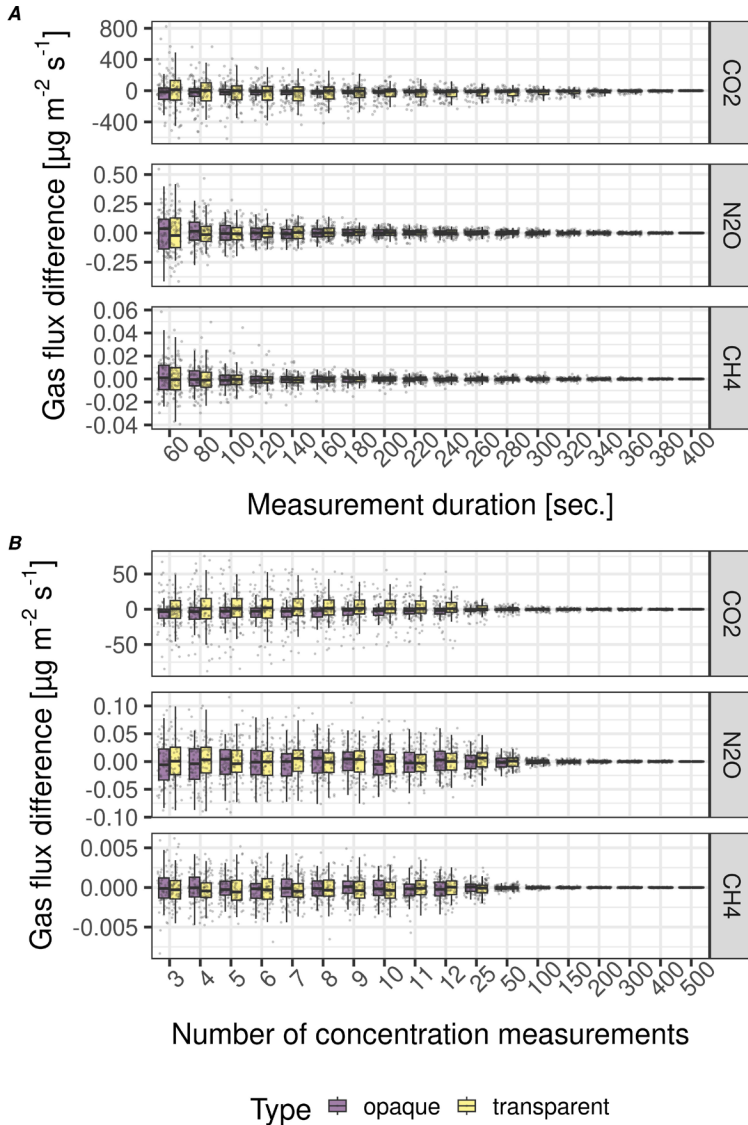


Figure 11. Box plots showing (A) differences between flux estimates of all measurement durations and flux estimates of the full 400 seconds (6:40 min.) of chamber closure duration and (B) differences between flux estimates per number of concentration measurements (*i.e.* number of concentration measurements < 500) and the flux estimate of the full dataset (*i.e.* number of concentration measurements = 500). Zero indicates no deviation from the median flux estimate of the full data set. Scattered dots represent individual data points. Transparent chamber measurements shown in yellow, opaque measurements in purple. Source: Paper II.

4.2.2 Influence of number of concentration measurements on flux estimate precision

Differences between flux estimates based on the reduced sets of data (<500 concentrations) and the full set (>500 concentrations) are shown in Figure 11B. A reduction in the number of concentrations led to a greater variation around the median flux, thus lowering the flux estimate precision for all three GHGs.

The proportion of fluxes in the reduced data sets (number of concentration measurements < 500) that were above the DL under the condition that the respective fluxes from the full data set (number of concentration measurements = 500) were below the DL revealed type 1 error abundance. Conversely, the proportion of fluxes from the reduced data sets that were below the DL under the condition that the respective fluxes from the full data set were above the DL revealed the type 2 error abundance. The CO₂ and CH₄ fluxes from the reduced data did not show evidence of type 1 errors or type 2 errors (Figure 12B). At three concentration measurements per N₂O flux, type 1 errors exceeded 5% for both the transparent and opaque measurements. The N₂O fluxes exceeded a type 2 error proportion of 5% at less than 250 and 325 concentration measurements for transparent and opaque chamber measurements, respectively (Figure 12B). This suggests that with the given flux magnitude at the study site and the measurement system used, the minimum number of concentration measurements per flux is between 250 and 325 for N₂O fluxes and for CO₂ and CH₄ three concentration measurements per flux would be sufficient to avoid significant type 1 or type 2 errors.

Using Equation 9 with MEF of 0.009 $\mu\text{g m}^{-2} \text{s}^{-1}$ and a measurement duration of 400 seconds at precision of $p = 3.8$ ppbv the minimum number of concentration measurements for N₂O fluxes was estimated to 308. With MEF for CH₄ of -0.0038 $\mu\text{g m}^{-2} \text{s}^{-1}$, the same measurement duration and $p = 0.37$ ppbv, the minimum number of concentrations was estimated to eight. Therefore, the minimum number of concentrations determined by Equation 9 for N₂O fluxes within the range of those determined by the type 2 error occurrence. For CH₄ fluxes, both methods deviated by five concentration measurements per flux.

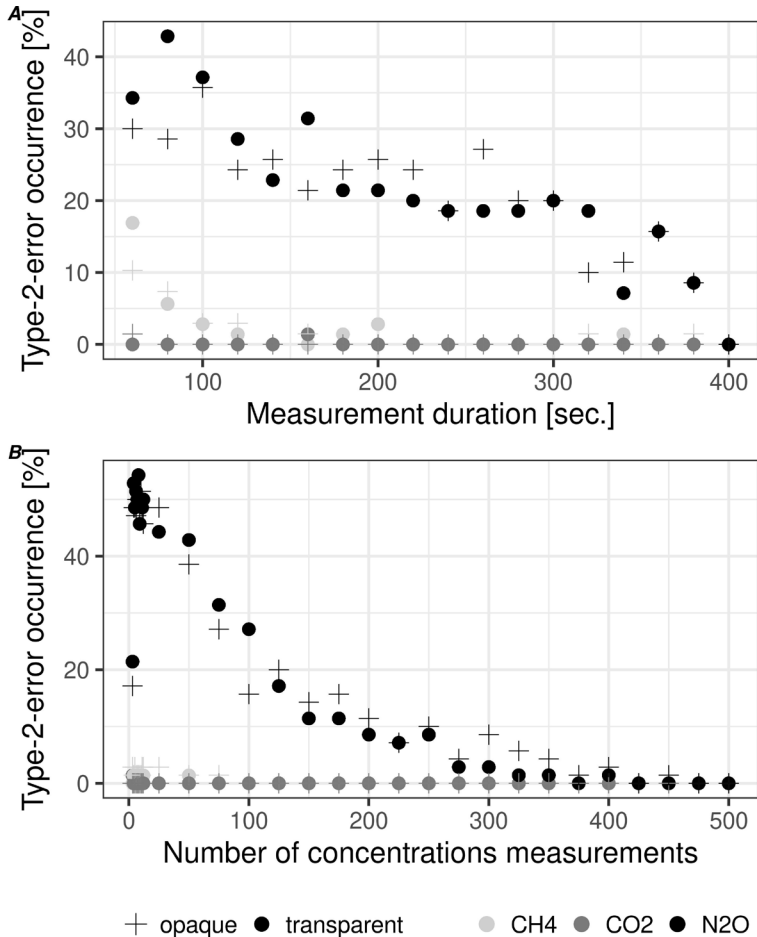


Figure 12. Relative type 2 error occurrence for carbon dioxide (CO₂), nitrous oxide (N₂O), and methane (CH₄) fluxes in transparent and opaque chamber measurements. (A) measurement duration and (B) number of concentration measurements per flux. Source: Paper II.

4.3 Paper III

The CL and SA site, both acted as net CO₂ sources over the whole measurement period from 1 January 2013 to 28 August 2019, with losses of 0.97 (±0.05) and 2.09 (±0.17) kg CO₂ m⁻² from the CL and SA site, respectively (Figure 13). Annual CO₂ losses during the period 1. January 2013 to 31. December 2018 were 0.16 kg CO₂ m⁻² yr⁻¹ at the CL site and 0.41

kg CO₂ m⁻² yr⁻¹ at the SA site. The different management regimes at the sites likely affected the inter-annual differences in flux dynamics between sites. For the CL site, effects of ploughing, disc cultivation and crop development early in the season were evident in the cumulative CO₂ fluxes (Figure 13). The SA site showed relatively consistent CO₂ flux dynamics, with little variation between years. This may be due to the extensive management regime, which consisted of an annual cut without biomass removal from 2015 onwards. In 2018, the biomass was removed during an animal feed shortage, which may have led to a higher CO₂ uptake in the following year. The summer of 2018 was the driest and warmest during the measurement period (Table 1), which impaired plant development at the SA site and led to lower CO₂ uptake (Figure 13).

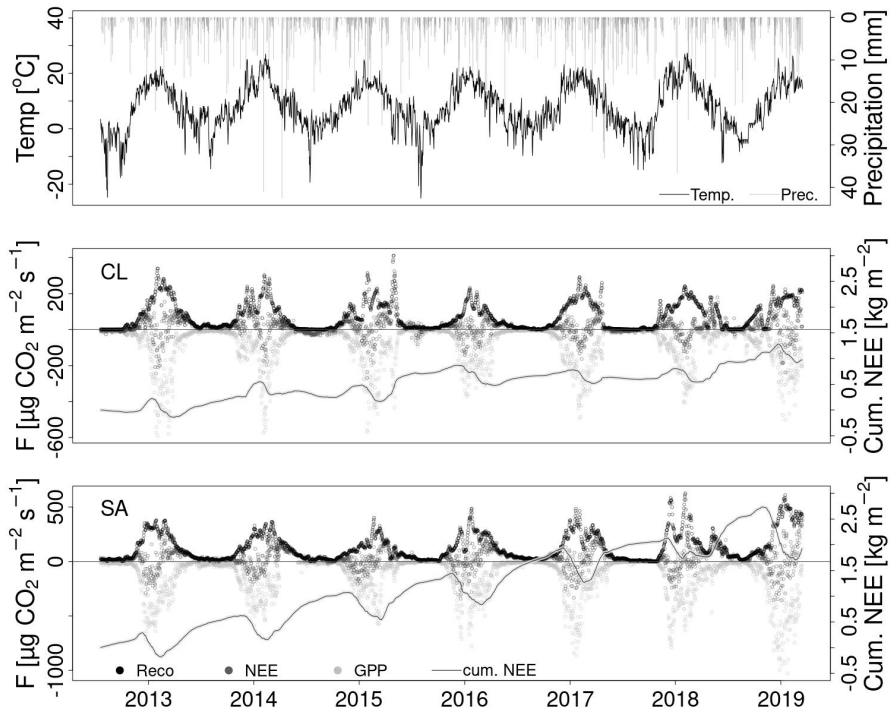


Figure 13. Mean daily precipitation and temperature (top panel) and mean daily carbon dioxide (CO₂) flux as net ecosystem exchange (NEE, dark grey), ecosystem respiration (R_{ECO}, black), gross primary production (GPP, light grey), and cumulative NEE flux (Cum. NEE) at the cultivated cropland (CL, centre panel) and set-aside grassland (SA, lower panel) during the study period 2013 to 2019. Source: adapted from Paper III.

During the growing seasons (May to August) of 2018 to 2020, transparent and opaque chamber measurements were conducted at both sites. Those resulted in mean NEE flux of -234.9 and -276.8 $\mu\text{g m}^{-2} \text{s}^{-1}$, mean R_{ECO} of 150.7 and 476.1 $\mu\text{g m}^{-2} \text{s}^{-1}$, and mean R_{SOIL} of 113.7 and 215.6 $\mu\text{g m}^{-2} \text{s}^{-1}$ at the CL and SA site, respectively (Table 2). Methane uptake was predominant at both sites, but higher at the SA site than at the CL site. However, 30.2% of CH_4 fluxes at the CL site and 1.8% of those at the SA site were below the DL of the instrument (Table S2 in Paper III). The N_2O fluxes were higher at the CL site from the transparent chamber measurements and the measurements on bare peat, while the fluxes from opaque chamber measurements were lower at the CL site compared with the SA site (Table 2). For N_2O , 70.8% of fluxes at the CL site and 50.0% at the SA site were below the DL of the instrumentation (Table S2 in Paper III).

The GHG balance for both sites was calculated using global warming potential based on 100 years (GWP_{100}) of 298 for N_2O and 34 for CH_4 and expressed in CO_2EQ (Myhre et al., 2013). At both sites, the GHG balance was dominated by CO_2 fluxes, while N_2O and CH_4 fluxes had only a minor influence (Table 2). The GHG source in terms of CO_2EQ was larger at the SA site for opaque chamber measurements and for the measurements on bare peat. The CO_2 uptake measured with the transparent chambers dominated the GHG balance, and thus the SA site was still a larger sink in terms of CO_2EQ even after accounting for the contributions of CH_4 and N_2O .

During the years 2018 to 2020, EC measurements were complemented by chamber measurements at both sites. Figure 14 shows a comparison of NEE during the summer months (May to August) of 2018 to 2020. Deviations between the two methods may be due to a mismatch in the source areas between the two systems or to recurring disturbance of the vegetation during the regular chamber measurements.

Table 2. Mean greenhouse gas (GHG) fluxes (carbon dioxide (CO₂), nitrous oxide (N₂O), and methane (CH₄)) during the summer months (May to August) 2018 to 2020 at the cultivated cropland site (CL) and set-aside grassland (SA), measured with transparent and opaque chambers, and on bare peat. Standard deviations (σ) and number of observations (n) are shown in brackets. GHG balance expressed in CO₂EQ. Source: adapted from Paper III.

Site	Type	CO ₂	N ₂ O	CH ₄	GHG balance
		Mean [$\mu\text{g m}^{-2} \text{s}^{-1}$] ($\pm\sigma$)	Mean [$\text{ng m}^{-2} \text{s}^{-1}$] ($\pm\sigma$)		CO ₂ EQ [$\mu\text{g m}^{-2} \text{s}^{-1}$]
CL	Transparent, with vegetation	-235.9 (± 348.3); $n = 119$	34.09 (± 54.65); $n = 116$	-3.46 (± 12.65); $n = 111$	-225.9
SA	Transparent, with vegetation	-276.8 (± 303.9); $n = 306$	8.45 (± 15.32); $n = 344$	-12.60 (± 7.54); $n = 344$	-274.7
CL	Opaque, with vegetation	150.7 (± 106.5); $n = 61$	5.73 (± 16.93); $n = 63$	-1.11 (± 18.22); $n = 59$	152.4
SA	Opaque, with vegetation	476.1 (± 218.0); $n = 290$	19.79 (± 112.1); $n = 290$	-15.71 (± 8.12); $n = 290$	481.4
CL	Bare peat	113.7 (± 119.9); $n = 87$	20.93 (± 30.61); $n = 84$	-2.24 (± 18.27); $n = 85$	119.8
SA	Bare peat	215.6 (± 195.9); $n = 196$	0.05 (± 15.01); $n = 196$	-12.73 (± 15.64); $n = 196$	215.2

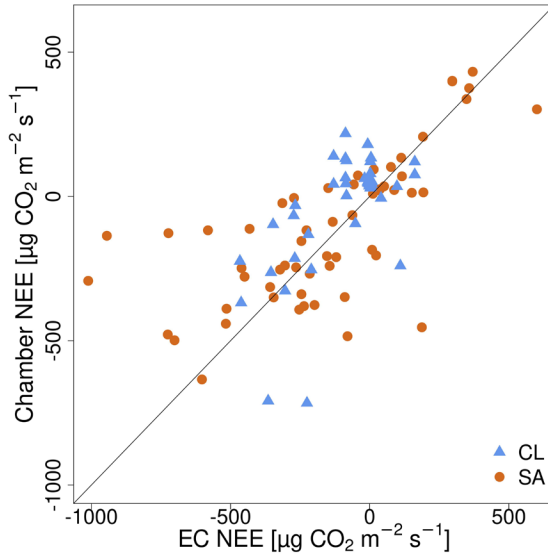


Figure 14. Comparison of the net ecosystem exchange (NEE) fluxes measured by eddy covariance (EC) and by transparent manual chambers at the cultivated cropland site (CL, blue triangles) and set-aside grassland site (SA, red dots). Solid line: $x=y$. Source: adapted from Paper III.

5. Discussion

5.1 Paper I

The results in Paper I indicated the measurement performance of the REA system was similar to that of the EC method for turbulent CO₂ and H₂O fluxes (see Figure 7 and Figure 8). Discrepancies between the two micrometeorological systems were observed in periods of low turbulent mixing (Figure 9), during which the EC system may be limited in the frequency response of its LI-6262 gas analyser and the REA system may lower the effect of single eddies contributing heavily to the EC covariance ($\overline{w'CO_2'}$), due to the representation of the vertical wind speed as σ_w . However, periods of low turbulent mixing are usually removed during standard post-processing of micrometeorological data by application of an ustar-filtering algorithm (Papale et al., 2006; Wutzler et al., 2018). While post-processing of raw data is possible with EC, it cannot be done with data from the REA system. Since the raw turbulence data from the sonic anemometer directly determine the sampling of updrafts and downdrafts, retrospective alterations are impossible. Thus, coordinate rotation must be performed on the basis of data obtained prior to measurement (e.g. a 30-minute mean wind vector). This implies that during periods of continuous and strong lateral wind, cross-contamination between flux components due to temporal sensor misalignment may lead to air sampling into the wrong reservoir.

In designing the REA system, emphasis was placed on a modular design and low power demand, so that the system can be assembled and installed easily in remote locations. Virtually all components were installed inside rugged cases, besides the analyser, and only connected by cabling and PTFE

tubing in a plug-and-play manner. Since all components run on 12 V DC, apart from the G2508 analyser, the system's power supply can be secured by *e.g.* solar panels and 12 V batteries. Several gas analysers based on 12 V DC power are now available and could be combined to measure many more non-sticky trace gases and some of their isotopes at remote locations. Another difference between the REA system compared with many previously described systems is the use of pressure boxes for sampling and evacuation of the sample reservoirs. This method was chosen to avoid contamination of the sample air due to pumps installed within the sample line, but involves a minor inconvenience in that the sample reservoirs are subjected to mechanical stress due to the sampling and evacuation cycles and need to be replaced at regular intervals. Furthermore, the 12 V pumps need to compensate for pressure drops due to leakages from the boxes that can occur during pressurised periods when the reservoirs are evacuated. A similar approach using pressure containers was developed by Haapanala et al. (2006) for filling sample reservoirs that were later analysed off-site. However, this REA system allows for continuous flux measurements on-site.

5.2 Paper II

The reliability of gas flux estimates is defined by the precision of the measurements system in relation to the flux magnitude. The low N₂O fluxes at the study site, in combination with the precision of the Picarro G2508 analyser for the same gas, resulted in considerable bias and large proportions of the measured fluxes being below the DL. On reducing the measurement duration or the number of concentration measurements per flux, the bias will increase and type 1 and type 2 errors occur more frequently. On the other hand, the CO₂ and CH₄ fluxes detected were large in relation to the system's DLs and little bias and low proportion of type 1 or type 2 errors were introduced by reducing the measurement duration to one minute or the number of concentration measurements down to three. The low N₂O fluxes in combination with analyser precision resulted in a large fraction (44%) of the N₂O fluxes being below the DL for the full dataset.

Extending the gas build-up phase within the chamber headspace by prolonging the measurement durations may be a good solution to improve the flux estimate by improving the signal-to-noise ratio and the DL (Parkin et al., 2012). However, when measuring several gas species in parallel,

attention must be paid to gases with high flux magnitudes (*e.g.* CO₂). A concentration increase in *e.g.* CO₂ within the headspace may lead to a change in the diffusion gradient between soil and headspace over time and make flux estimates less reliable (Duran and Kucharik, 2013; Kroon et al., 2008). Using only the initial linear change in headspace concentration of CO₂ allows application of a linear flux calculation scheme and reduces the bias due to a changing diffusion gradient over time. At the same time, the N₂O flux can be calculated using the complete measurement duration, which improves the flux estimate precision for N₂O (Courtois et al., 2019). Applied to the data in Paper II, this would mean that using only the first 60 seconds of measurement, would be sufficient to obtain a flux that is well above the DL of the system for CO₂. At least 80 seconds would be sufficient for CH₄ and at least 380 seconds for N₂O. Measuring low N₂O fluxes is a challenge, so harmonising the equipment and the flux measurement strategy is important. Equation 9 can be helpful in determining the minimum measurement duration for N₂O or CH₄ flux measurements based on the expected flux magnitude and the precision of the analyser.

With the gas flux magnitudes prevailing at the field sites and the precision of the sampling system, three concentration samples were sufficient to achieve CO₂ fluxes above the system's DL at a measurement duration of 400 seconds. For CH₄, a minimum of three to eight samples were sufficient. For the low N₂O fluxes, at least 250 concentration measurements were needed to obtain N₂O fluxes above the DL. Thus, in the case of Paper II, the general recommendation of four to five concentration samples (Sander and Wassmann, 2014) would be too few for estimating reliable N₂O fluxes. With four samples, measurement duration of 34 minutes would be needed according to Equation 9. However, in a more heterogeneous environment, taking more chamber measurements may be preferable at the expense of number of concentrations per flux measurement, as suggested by Jungkunst et al. (2018) and Levy et al. (2011), in order to find the optimum between individual and spatial flux uncertainty.

When an automated chamber system with a fast gas analyser is used, there usually is no reason to reduce the number of concentration measurements below the available maximum. However, simultaneous sampling of multiple chambers facilitated by an air circulation system aided by a manifold to separate sample air and bypass air from individual chambers, may help to enhance the spatial and temporal resolution of GHG flux estimations. This

approach allows for efficient GHG emission scanning by striking a balanced compromise between chamber measurement duration, number of concentration measurements per flux and number of simultaneously sampled chambers.

5.3 Paper III

Using an EC approach, Hadden and Grelle (2017) examined CO₂ fluxes at the same two sites as in Paper III during the period 2012 to 2016 and found that the CL site acted as a small CO₂ sink (-0.2 kg CO₂ m⁻²) and the SA site as a small source (0.2 kg CO₂ m⁻²) during this period. However, in Paper III, both sites were found to be sources of CO₂ (0.16 kg CO₂ m⁻² yr⁻¹ at the CL site and 0.41 kg CO₂ m⁻² yr⁻¹ at the SA site). This discrepancy likely originated from the different data post-processing procedures applied. Hadden and Grelle (2017) excluded unreliable data originating from instrument failures or ice formation on the sonic anemometers, outliers and negative CO₂ fluxes at night. Paper III additionally applied a more rigorous outlier detection method (median absolute deviation) and an ustar-filtering algorithm (Papale et al., 2006; Wutzler et al., 2018). For gap-filling, Hadden and Grelle (2017) used linear interpolation for 30-minute data gaps in combination with the mean diurnal course method (Falge et al., 2001). Paper III used the marginal distribution sampling algorithm (Reichstein et al., 2005; Wutzler et al., 2018). Some discrepancies in the results may also be explained by differences in measurement duration (mid-2012 to end-2016 Hadden and Grelle (2017) and beginning-2013 to mid-2019 in Paper III). The change in agricultural management at both sites may also have influenced the results, where mouldboard ploughing at the CL site was replaced by disc cultivation in 2016 and yearly grass cuts were introduced at the SA site in 2015.

Over two consecutive years, Lohila et al. (2004) measured NEE by EC in a drained Finnish peatland producing barley with under-sown grass in the first year and grass only in the second year. They observed annual net CO₂ losses of 0.77 kg CO₂ m⁻² yr⁻¹ for barley in the first year and 0.29 kg CO₂ m⁻² yr⁻¹ for grass in the second year. These cumulative emissions exceeded those in Paper III, possibly due to a thicker peat layer (40 to 60 cm) at the Finnish site than at the SA or CL site (25 and 34 cm, respectively). For a shallow agricultural peat in Finland cropped with grass silage, Gerin et al.

(2023) measured NEE using EC and found higher cumulative annual emissions than in Paper III, even though peat thickness was somewhat less (15-30 cm) than at the SA site in Paper III. This discrepancy may be due to a management effect related to the cutting regime, since the Finnish grass silage crop was cut twice a year, which led to CO₂ emissions peaks directly afterwards, while grass at the SA site was cut only once a year.

However, peat layer thickness and management are not the only variables that may affect C fluxes. In a study comprising NEE flux measurements by EC at 16 locations in the UK and Ireland, Evans et al. (2021) found no overall effect of peatland management, but a strong influence of effective water table depth (*i.e.* thickness of the aerated peat layer). Thus, agricultural peatland management factors such as ploughing intensity or crop type may have explanatory relevance for differences found in some site comparisons (Kløve et al., 2017), but effective water table depth seems to have an overriding effect on CO₂ emissions from temperate peatlands in general (Evans et al., 2021). At the study sites in Paper III, the water table is located within the mineral subsoil below the peat for most of the year, so the effective water table depth is largely defined by the peat layer thickness. Thus, the higher cumulative CO₂ emissions at the SA site may be explained by its lower effective water table.

Measurements of C exports were not part of the work in this thesis. However, a rough estimation of C exports, in terms of CO₂ due to herbivory and harvest (CO₂_{HARV/HERB}) was made. Based on personal communication with the farmer, grain yield at the CL site were estimated to 0.2 kg m⁻² yr⁻¹ (Olsson, pers. comm.), except for the fallow period in 2016 (no yield) and when barley was cultivated and harvested in 2018 (yield 0.37 kg m⁻²). Thus, potential grain yield was estimated to be 1.17 kg m⁻² for the period 2013 to 2019. It was assumed that herbivory during autumn and winter by deer, wild boar, moose, and birds accounted for 80% of the potential grain yield, excluding the years 2016 and 2018 for the above-mentioned reasons. Moreover, correction was made for grain water content of 15% and it was assumed that roughly half of the biomass consumed by wildlife was returned to the site by excreta. A biomass-to-C ratio of 0.45 was assumed (Hicke et al., 2004). Resulting in an annual CO₂ loss of about 0.16 kg CO₂ m⁻² yr⁻¹. Herbivory at the SA site was not observed systematically. Therefore, the estimation by Hadden and Grelle (2017) of an annual C loss due to herbivory of 0.03 kg C m⁻² yr⁻¹ (0.11 kg CO₂ m⁻² yr⁻¹) was used. With the harvest in

2018, an additional $0.45 \text{ kg CO}_2 \text{ m}^{-2}$ was exported as hay. Thus, over the period from 2013 to 2019 the annual C export, expressed in CO_2 was estimated to $0.167 \text{ kg m}^{-2} \text{ yr}^{-1}$. Overall, the annual CO_2 emissions as the sum of NEE and $\text{CO}_{2_HARV/HERB}$, summed up to $0.32 \text{ kg CO}_2 \text{ m}^{-2} \text{ yr}^{-1}$ at the CL site and to $0.58 \text{ kg CO}_2 \text{ m}^{-2} \text{ yr}^{-1}$ at the SA site. On including the effects of harvest and herbivory, the CO_2 budget of the CL site remained below that of the SA site. However, $\text{CO}_{2_HARV/HERB}$ was based on rough estimates rather than measurements, so the calculations only provide an indication of CO_2 losses at both sites.

Based on the chamber measurements, and in agreement with Berglund et al. (2021), there were higher CO_2 fluxes (uptake, R_{ECO} , and R_{SOIL}), lower N_2O emissions (transparent and bare peat), and stronger CH_4 uptake (under all conditions) at the SA site compared with the CL site. The GHG budgets calculated from the GWP_{100} of each gas, were also comparable to those reported by Berglund et al. (2021), with the exception of the vegetated measurements at the SA site. The deviation in the vegetated measurements was likely because in the study by Berglund et al. (2021) the vegetation needed to be trimmed due to the height limit defined by the chambers used, the higher chambers used in Paper III meant that the vegetation could be left intact.

During a period of more than six years, both the CL and the SA site acted as CO_2 sources, with the SA site emitting more CO_2 to the atmosphere than the CL site. Thus, there was no evidence indicating that setting-aside agricultural peatland reduces its CO_2 emissions.

6. Conclusions and future perspectives

The new REA system developed in this thesis was running reliably during summer and winter months in the Nordic climate and produced CO₂ and H₂O fluxes that were in good agreement with those of an EC system operated in parallel. The determined DLs found for N₂O and CH₄ fluxes and the identical sampling technology confirmed that the REA system can capture N₂O and CH₄ fluxes reliably. The modular design of the system proved to be very practical, allowing for fast and easy installation in the field. Passive sampling by pressure containers ensured a constant sample flow rate into the reservoirs, while contaminant sources like pumps were eliminated from the sample flow. Occasionally the sample reservoirs needed replacing, due to cracks developing inside the bags after many sampling-evacuation cycles. Another challenge in the sampling system was leakages from the pressure containers during the reservoir evacuation phase. This did not affect air sampling quality, but led to an increase in operational time of the pumps to compensate for the resulting pressure drops. Overall, the presented REA system measures GHG fluxes continuously above terrestrial ecosystems and offers the possibility of using several analysers to measure many more atmospheric tracers and even their isotopic composition. With the modular design and the option of using low-power gas analysers, it can be installed off-grid and in remote locations.

Measurement duration and number of concentration measurements influenced the uncertainty of individual flux estimates. This finding can be used to optimise flux measurement strategies using manual chambers, especially by applying Equation 9 to determine the optimal measurement duration and number of concentration measurements needed in relation to the expected flux magnitude and analyser precision for each chamber measurement. When low N₂O flux magnitudes are expected and CO₂ fluxes

are determined simultaneously, only the initial linear increase in CO₂ concentration should be used for CO₂ flux calculation and extended measurement duration should be used to determine reliable N₂O fluxes. In this way, the influence of long measurement duration on the diffusion gradient of CO₂ can be reduced and, and at the same time, N₂O fluxes well above the system DL can be achieved.

There was no evidence to suggest that setting-aside agricultural peatland will reduce its CO₂ emissions. In fact, over a measurement period of more than six years, set-aside grassland (SA) acted as a larger source of CO₂ than an adjacent cultivated cropland (CL). The SA site showed elevated levels of respiratory CO₂ losses, photosynthetic CO₂ assimilation, and CH₄ uptake compared with the CL site, while N₂O emissions from the CL site exceeded those from the SA site (CH₄ and N₂O made a minor contributions to GHG balance at both sites). These results suggest that the present incentives for setting-aside agricultural peatlands are in need of reassessment if a reduction of GHG emissions is aspired. Thus, direct payments under the Common Agricultural Policy of the EU (EU Regulation No 1307/2013, 2013) for setting-aside agricultural peatlands are likely to be an ineffective means to achieve CO₂ emission reductions if the peatlands remain in a drained state. Therefore, re-evaluation of present policies and incentives that aim at supporting set-aside farmland on drained peat is needed.

To improve our understanding of GHG flux dynamics of drained peatland ecosystems, estimating complete C and N balances, including losses due to harvest, herbivory, and seepage, can be of great value. Multi-seasonal and continuous GHG flux measurements at several peatland sites under different land use and management intensities, ideally paired with rewetting experiments, would provide valuable insights into management alternatives for agricultural peatlands aimed at reducing GHG emissions.

References

- Aubinet, M., Grelle, A., Ibrom, A., Rannik, Ü., Moncrieff, J., Foken, T., Kowalski, A.S., Martin, P.H., Berbigier, P., Bernhofer, Ch., Clement, R., Elbers, J., Granier, A., Grünwald, T., Morgenstern, K., Pilegaard, K., Rebmann, C., Snijders, W., Valentini, R., Vesala, T., 1999. Estimates of the Annual Net Carbon and Water Exchange of Forests: The EUROFLUX Methodology, in: *Advances in Ecological Research*. Elsevier, pp. 113–175. [https://doi.org/10.1016/S0065-2504\(08\)60018-5](https://doi.org/10.1016/S0065-2504(08)60018-5)
- Berglund, Ö., 1996. Cultivated organic soils in Sweden: properties and amelioration (PhD thesis). Sveriges lantbruksuniversitet, Uppsala, Sweden.
- Berglund, Ö., Berglund, K., 2010. Distribution and cultivation intensity of agricultural peat and gyttja soils in Sweden and estimation of greenhouse gas emissions from cultivated peat soils. *Geoderma* 154, 173–180. <https://doi.org/10.1016/j.geoderma.2008.11.035>
- Berglund, Ö., Kätterer, T., Meurer, K.H.E., 2021. Emissions of CO₂, N₂O and CH₄ From Cultivated and Set Aside Drained Peatland in Central Sweden. *Front. Environ. Sci.* 9, 630721. <https://doi.org/10.3389/fenvs.2021.630721>
- Beverland, I.J., Ónéill, D.H., Scott, S.L., Moncrieff, J.B., 1996. Design, construction and operation of flux measurement systems using the conditional sampling technique. *Atmospheric Environment* 30, 3209–3220. [https://doi.org/10.1016/1352-2310\(96\)00010-6](https://doi.org/10.1016/1352-2310(96)00010-6)
- Bonn, A., Allott, T., Evans, M., Joosten, H., Stoneman, R., 2016. Peatland restoration and ecosystem services: science, policy, and practice, *Ecological reviews*. Cambridge university press, Cambridge.
- Bräuer, S.L., Basiliko, N., Siljanen, H.M.P., Zinder, S.H., 2020. Methanogenic archaea in peatlands. *FEMS Microbiology Letters* 367, fnaa172. <https://doi.org/10.1093/femsle/fnaa172>
- Businger, J.A., Oncley, S.P., 1990. Flux Measurement with Conditional Sampling. *Journal of Atmospheric and Oceanic Technology* 7, 349–352. [https://doi.org/10.1175/1520-0426\(1990\)007<0349:FMWCS>2.0.CO;2](https://doi.org/10.1175/1520-0426(1990)007<0349:FMWCS>2.0.CO;2)
- Butterbach-Bahl, K., Baggs, E.M., Dannenmann, M., Kiese, R., Zechmeister-Boltenstern, S., 2013. Nitrous oxide emissions from soils: how well do we understand the processes and their controls? *Philosophical Transactions of the Royal Society B: Biological Sciences* 368, 20130122–20130122. <https://doi.org/10.1098/rstb.2013.0122>
- Christensen, T.R., Friborg, T., Byrne, K., Chojnicki, B., Drösler, M., Freibauer, A., Frolking, S., Lindroth, A., Mailhammer, J., Malmer, N., Selin, S., Turunen,

- J., Valentini, R., Zetterberg, L., Vandewalle, M., 2004. EU Peatlands: Current Carbon Stocks and Trace Gas Fluxes (No. 4), Concerted action: Synthesis of the European Greenhouse Gas Budget. Geosphere-Biosphere Centre, Univ. of Lund, Sweden.
- Courtois, E.A., Stahl, C., Burban, B., Van Den Berge, J., Berveiller, D., Bréchet, L., Soong, J.L., Arriga, N., Peñuelas, J., Janssens, I.A., 2019. Automatic high-frequency measurements of full soil greenhouse gas fluxes in a tropical forest. *Biogeosciences* 16, 785–796. <https://doi.org/10.5194/bg-16-785-2019>
- Desjardins, R.L., Pattey, E., Smith, W.N., Worth, D., Grant, B., Srinivasan, R., MacPherson, J.I., Mauder, M., 2010. Multiscale estimates of N₂O emissions from agricultural lands. *Agricultural and Forest Meteorology* 150, 817–824. <https://doi.org/10.1016/j.agrformet.2009.09.001>
- Duran, B.E.L., Kucharik, C.J., 2013. Comparison of Two Chamber Methods for Measuring Soil Trace-Gas Fluxes in Bioenergy Cropping Systems. *Soil Science Society of America Journal* 77, 1601–1612. <https://doi.org/10.2136/sssaj2013.01.0023>
- Eniro.se, 2023. Satellite image of research site. <https://kartor.eniro.se/m/kaKq4>
- EU Regulation No 1307/2013, 2013. REGULATION (EU) No 1307/2013 OF THE EUROPEAN PARLIAMENT AND OF THE COUNCIL.
- Evans, C.D., Peacock, M., Baird, A.J., Artz, R.R.E., Burden, A., Callaghan, N., Chapman, P.J., Cooper, H.M., Coyle, M., Craig, E., Cumming, A., Dixon, S., Gauci, V., Grayson, R.P., Helfter, C., Heppell, C.M., Holden, J., Jones, D.L., Kaduk, J., Levy, P., Matthews, R., McNamara, N.P., Misselbrook, T., Oakley, S., Page, S.E., Rayment, M., Ridley, L.M., Stanley, K.M., Williamson, J.L., Worrall, F., Morrison, R., 2021. Overriding water table control on managed peatland greenhouse gas emissions. *Nature*. <https://doi.org/10.1038/s41586-021-03523-1>
- Falge, E., Baldocchi, D., Olson, R., Anthoni, P., Aubinet, M., Bernhofer, C., Burba, G., Ceulemans, R., Clement, R., Dolman, H., Granier, A., Gross, P., Grünwald, T., Hollinger, D., Jensen, N.-O., Katul, G., Keronen, P., Kowalski, A., Lai, C.T., Law, B.E., Meyers, T., Moncrieff, J., Moors, E., Munger, J.W., Pilegaard, K., Rannik, Ü., Rebmann, C., Suyker, A., Tenhunen, J., Tu, K., Verma, S., Vesala, T., Wilson, K., Wofsy, S., 2001. Gap filling strategies for defensible annual sums of net ecosystem exchange. *Agricultural and Forest Meteorology* 107, 43–69. [https://doi.org/10.1016/S0168-1923\(00\)00225-2](https://doi.org/10.1016/S0168-1923(00)00225-2)
- Frolking, S., Roulet, N.T., 2007. Holocene radiative forcing impact of northern peatland carbon accumulation and methane emissions. *Global Change Biol* 13, 1079–1088. <https://doi.org/10.1111/j.1365-2486.2007.01339.x>
- Fuss, R., Hueppi, R., Asger, R., 2020. gasfluxes: Greenhouse gas flux calculation from chamber measurements.

- Gaman, A., Rannik, Ü., Aalto, P., Pohja, T., Siivola, E., Kulmala, M., Vesala, T., 2004. Relaxed Eddy Accumulation System for Size-Resolved Aerosol Particle Flux Measurements. *Journal of Atmospheric and Oceanic Technology* 21, 933–943. [https://doi.org/10.1175/1520-0426\(2004\)021<0933:REASFS>2.0.CO;2](https://doi.org/10.1175/1520-0426(2004)021<0933:REASFS>2.0.CO;2)
- Gerin, S., Vekuri, H., Liimatainen, M., Tuovinen, J.-P., Kekkonen, J., Kulmala, L., Laurila, T., Linkosalmi, M., Liski, J., Joki-Tokola, E., Lohila, A., 2023. Two contrasting years of continuous N₂O and CO₂ fluxes on a shallow-peated drained agricultural boreal peatland. *Agricultural and Forest Meteorology* 341, 109630. <https://doi.org/10.1016/j.agrformet.2023.109630>
- Grelle, A., Keck, H., 2021. Affordable relaxed eddy accumulation system to measure fluxes of H₂O, CO₂, CH₄ and N₂O from ecosystems. *Agricultural and Forest Meteorology* 307, 108514. <https://doi.org/10.1016/j.agrformet.2021.108514>
- Grønlund, A., Hauge, A., Hovde, A., Rasse, D.P., 2008. Carbon loss estimates from cultivated peat soils in Norway: a comparison of three methods. *Nutr Cycl Agroecosyst* 81, 157–167. <https://doi.org/10.1007/s10705-008-9171-5>
- Haapanala, S., Rinne, J., Pystynen, K.-H., Hellén, H., Hakola, H., Riutta, T., 2006. Measurements of hydrocarbon emissions from a boreal fen using the REA technique. *Biogeosciences* 3, 103–112. <https://doi.org/10.5194/bg-3-103-2006>
- Hadden, D., Grelle, A., 2017. The impact of cultivation on CO₂ and CH₄ fluxes over organic soils in Sweden. *Agricultural and Forest Meteorology* 243, 1–8. <https://doi.org/10.1016/j.agrformet.2017.05.002>
- Hargreaves, K.J., Wienhold, F.G., Klemetsson, L., Arah, J.R.M., Beverland, I.J., Fowler, D., Galle, B., Griffith, D.W.T., Skiba, U., Smith, K.A., Welling, M., Harris, G.W., 1996. Measurement of nitrous oxide emission from agricultural land using micrometeorological methods. *Atmospheric Environment* 30, 1563–1571. [https://doi.org/10.1016/1352-2310\(95\)00468-8](https://doi.org/10.1016/1352-2310(95)00468-8)
- Helbig, M., Waddington, J.M., Alekseychik, P., Amiro, B., Aurela, M., Barr, A.G., Black, T.A., Carey, S.K., Chen, J., Chi, J., Desai, A.R., Dunn, A., Euskirchen, E.S., Flanagan, L.B., Friborg, T., Garneau, M., Grelle, A., Harder, S., Heliasz, M., Humphreys, E.R., Ikawa, H., Isabelle, P.-E., Iwata, H., Jassal, R., Korkiakoski, M., Kurbatova, J., Kutzbach, L., Lapshina, E., Lindroth, A., Löfvenius, M.O., Lohila, A., Mammarella, I., Marsh, P., Moore, P.A., Maximov, T., Nadeau, D.F., Nicholls, E.M., Nilsson, M.B., Ohta, T., Peichl, M., Petrone, R.M., Prokushkin, A., Quinton, W.L., Roulet, N., Runkle, B.R.K., Sonnentag, O., Strachan, I.B., Taillardat, P., Tuittila, E.-S., Tuovinen, J.-P., Turner, J., Ueyama, M., Varlagin, A., Vesala, T., Wilmking, M., Zyrianov, V., Schulze, C., 2020. The biophysical climate

- mitigation potential of boreal peatlands during the growing season. *Environ. Res. Lett.* 15, 104004. <https://doi.org/10.1088/1748-9326/abab34>
- Hicke, J.A., Lobell, D.B., Asner, G.P., 2004. Cropland Area and Net Primary Production Computed from 30 Years of USDA Agricultural Harvest Data. *Earth Interact.* 8, 1–20. [https://doi.org/10.1175/1087-3562\(2004\)008<0001:CAANPP>2.0.CO;2](https://doi.org/10.1175/1087-3562(2004)008<0001:CAANPP>2.0.CO;2)
- Holden, J., Chapman, P.J., Labadz, J.C., 2004. Artificial drainage of peatlands: hydrological and hydrochemical process and wetland restoration. *Progress in Physical Geography: Earth and Environment* 28, 95–123. <https://doi.org/10.1191/0309133304pp403ra>
- Hüppi, R., Felber, R., Krauss, M., Six, J., Leifeld, J., Fuß, R., 2018. Restricting the nonlinearity parameter in soil greenhouse gas flux calculation for more reliable flux estimates. *PLoS ONE* 13, e0200876. <https://doi.org/10.1371/journal.pone.0200876>
- Hutchinson, G.L., Mosier, A.R., 1981. Improved Soil Cover Method for Field Measurement of Nitrous Oxide Fluxes. *Soil Science Society of America Journal* 45, 311–316. <https://doi.org/10.2136/sssaj1981.03615995004500020017x>
- IPCC, 2019. *Climate Change and Land: an IPCC special report on climate change, desertification, land degradation, sustainable land management, food security, and greenhouse gas fluxes in terrestrial ecosystems* [P.R. Shukla, J. Skea, E. Calvo Buendia, V. Masson-Delmotte, H.-O. Pörtner, D. C. Roberts, P. Zhai, R. Slade, S. Connors, R. van Diemen, M. Ferrat, E. Haughey, S. Luz, S. Neogi, M. Pathak, J. Petzold, J. Portugal Pereira, P. Vyas, E. Huntley, K. Kissick, M. Belkacemi, J. Malley, (eds.)]. Cambridge University Press, Cambridge, UK and New York, NY, USA, 896 pp. <https://doi.org/10.1017/9781009157988>
- Jackson R.B., Lajtha, K., Crow, S.E., Hugelius, G., Kramer, M.G., Piñeiro, G., 2017. The Ecology of Soil Carbon: Pools, Vulnerabilities, and Biotic and Abiotic Controls. *Annual Review of Ecology, Evolution, and Systematics* 2017 48:1, 419-445
- Joosten, H., Clarke, D., 2002. *Wise use of mires and peatland- Background and prinyiples including a framework for decision-making.*
- Jungkunst, H.F., Meurer, K.H.E., Jurasinski, G., Niehaus, E., Günther, A., 2018. How to best address spatial and temporal variability of soil-derived nitrous oxide and methane emissions. *J. Plant Nutr. Soil Sci.* 181, 7–11. <https://doi.org/10.1002/jpln.201700607>
- Kasimir-Klemedtsson, Å., Klemedtsson, L., Berglund, K., Martikainen, P., Silvola, J., Oenema, O., 1997. Greenhouse gas emissions from farmed organic soils: a review. *Soil Use & Management* 13, 245–250. <https://doi.org/10.1111/j.1475-2743.1997.tb00595.x>

- Kløve, B., Berglund, K., Berglund, Ö., Weldon, S., Maljanen, M., 2017. Future options for cultivated Nordic peat soils: Can land management and rewetting control greenhouse gas emissions? *Environmental Science & Policy* 69, 85–93. <https://doi.org/10.1016/j.envsci.2016.12.017>
- Kroon, P.S., Hensen, A., van den Bulk, W.C.M., Jongejan, P.A.C., Vermeulen, A.T., 2008. The importance of reducing the systematic error due to non-linearity in N₂O flux measurements by static chambers. *Nutr Cycl Agroecosyst* 82, 175–186. <https://doi.org/10.1007/s10705-008-9179-x>
- Kutzbach, L., Schneider, J., Sachs, T., Giebels, M., Nykänen, H., Shurpali, N.J., Martikainen, P.J., Alm, J., Wilmking, M., 2007. CO₂ flux determination by closed-chamber methods can be seriously biased by inappropriate application of linear regression. *Biogeosciences* 4, 1005–1025. <https://doi.org/10.5194/bg-4-1005-2007>
- Lai, D.Y.F., 2009. Methane Dynamics in Northern Peatlands: A Review. *Pedosphere* 19, 409–421.
- Leifeld, J., Menichetti, L., 2018. The underappreciated potential of peatlands in global climate change mitigation strategies. *Nat Commun* 9, 1071. <https://doi.org/10.1038/s41467-018-03406-6>
- Leppelt, T., Dechow, R., Gebbert, S., Freibauer, A., Lohila, A., Augustin, J., Drösler, M., Fiedler, S., Glatzel, S., Höper, H., Järveoja, J., Lærke, P.E., Maljanen, M., Mander, Ü., Mäkiranta, P., Minkkinen, K., Ojanen, P., Regina, K., Strömngren, M., 2014. Nitrous oxide emission budgets and land-use-driven hotspots for organic soils in Europe. *Biogeosciences* 11, 6595–6612. <https://doi.org/10.5194/bg-11-6595-2014>
- Levy, P.E., Gray, A., Leeson, S.R., Gaiawyn, J., Kelly, M.P.C., Cooper, M.D.A., Dinsmore, K.J., Jones, S.K., Sheppard, L.J., 2011. Quantification of uncertainty in trace gas fluxes measured by the static chamber method. *European Journal of Soil Science* 62, 811–821. <https://doi.org/10.1111/j.1365-2389.2011.01403.x>
- Lohila, A., Aurela, M., Tuovinen, J.-P., Laurila, T., 2004. Annual CO₂ exchange of a peat field growing spring barley or perennial forage grass. *J. Geophys. Res.* 109, D18116. <https://doi.org/10.1029/2004JD004715>
- Lundegårdh, H., 1927. Carbon dioxide evolution of soil and crop growth. *Soil Science* 23, 417–453.
- Maljanen, M., Hytönen, J., Mäkiranta, P., Alm, J., Minkkinen, K., Laine, J., Martikainen, P.J., 2007. Greenhouse gas emissions from cultivated and abandoned organic croplands in Finland. *Boreal Env. Res.* 12, 133–140.
- Maljanen, M., Sigurdsson, B.D., Guðmundsson, J., Óskarsson, H., Huttunen, J.T., Martikainen, P.J., 2010. Greenhouse gas balances of managed peatlands in the Nordic countries – present knowledge and gaps. *Biogeosciences* 7, 2711–2738. <https://doi.org/10.5194/bg-7-2711-2010>

- Myhre, G., Shindell, D., Bréon, F.-M., Collins, W., Fuglestedt, J., Huang, J., Koch, D., Lamarque, J.-F., Lee, D., Mendoza, B., Nakajima, T., Robock, A., Stephens, G., Takemura, T., Zhang, H., 2013. Anthropogenic and Natural Radiative Forcing, in: Stocker, T.F., Qin, D., Plattner, G.-K., Tignor, M., Allen, S.K., Boschung, J., Nauels, A., Xia, Y., Bex, V., Midgley, P.M. (Eds.), *Climate Change 2013: The Physical Science Basis. Contribution of Working Group I to the Fifth Assessment Report of the Intergovernmental Panel on Climate Change*. Cambridge University Press, Cambridge, United Kingdom and New York, NY, USA.
- Nerman, G., 1898. Temnarens sänkning. *Svenska Mosskulturföreningens tidskrift* 61–88.
- Olsson, pers. Comm. Communication with Farmer about yield and yield loss due to wildlife.
- Osterwalder, S., Fritsche, J., Alewell, C., Schmutz, M., Nilsson, M.B., Jocher, G., Sommar, J., Rinne, J., Bishop, K., 2016. A dual-inlet, single detector relaxed eddy accumulation system for long-term measurement of mercury flux. *Atmospheric Measurement Techniques* 9, 509–524. <https://doi.org/10.5194/amt-9-509-2016>
- Papale, D., Reichstein, M., Aubinet, M., Canfora, E., Bernhofer, C., Kutsch, W., Longdoz, B., Rambal, S., Valentini, R., Vesala, T., Yakir, D., 2006. Towards a standardized processing of Net Ecosystem Exchange measured with eddy covariance technique: algorithms and uncertainty estimation. *Biogeosciences* 3, 571–583. <https://doi.org/10.5194/bg-3-571-2006>
- Parkin, T.B., Venterea, R.T., Hargreaves, S.K., 2012. Calculating the Detection Limits of Chamber-based Soil Greenhouse Gas Flux Measurements. *Journal of Environment Quality* 41, 705. <https://doi.org/10.2134/jeq2011.0394>
- Pattey, E., Edwards, G.C., Desjardins, R.L., Pennock, D.J., Smith, W., Grant, B., MacPherson, J.I., 2007. Tools for quantifying N₂O emissions from agroecosystems. *Agricultural and Forest Meteorology* 142, 103–119. <https://doi.org/10.1016/j.agrformet.2006.05.013>
- Pedersen, A.R., Petersen, S.O., Schelde, K., 2010. A comprehensive approach to soil-atmosphere trace-gas flux estimation with static chambers. *European Journal of Soil Science* 61, 888–902. <https://doi.org/10.1111/j.1365-2389.2010.01291.x>
- R Core Team, 2023. R: A Language and Environment for Statistical Computing.
- R Core Team, 2020. R: A Language and Environment for Statistical Computing.
- Reichstein, M., Falge, E., Baldocchi, D., Papale, D., Aubinet, M., Berbigier, P., Bernhofer, C., Buchmann, N., Gilmanov, T., Granier, A., Grunwald, T., Havrankova, K., Ilvesniemi, H., Janous, D., Knohl, A., Laurila, T., Lohila, A., Loustau, D., Matteucci, G., Meyers, T., Miglietta, F., Ourcival, J.-M., Pumpanen, J., Rambal, S., Rotenberg, E., Sanz, M., Tenhunen, J., Seufert, G., Vaccari, F., Vesala, T., Yakir, D., Valentini, R., 2005. On the separation

- of net ecosystem exchange into assimilation and ecosystem respiration: review and improved algorithm. *Global Change Biol* 11, 1424–1439. <https://doi.org/10.1111/j.1365-2486.2005.001002.x>
- Ren, X., Sanders, J.E., Rajendran, A., Weber, R.J., Goldstein, A.H., Pusede, S.E., Browne, E.C., Min, K.-E., Cohen, R.C., 2011. A relaxed eddy accumulation system for measuring vertical fluxes of nitrous acid. *Atmos. Meas. Tech.* 4, 2093–2103. <https://doi.org/10.5194/amt-4-2093-2011>
- Riederer, M., Hübner, J., Ruppert, J., Brand, W.A., Foken, T., 2014. Prerequisites for application of hyperbolic relaxed eddy accumulation on managed grasslands and alternative net ecosystem exchange flux partitioning. *Atmospheric Measurement Techniques* 7, 4237–4250. <https://doi.org/10.5194/amt-7-4237-2014>
- Ritchie, H., 2020. Climate change and flying: what share of global CO₂ emissions come from aviation? [WWW Document]. Our World in Data. URL <https://ourworldindata.org/co2-emissions-from-aviation> (accessed 8.15.23).
- Sander, B.O., Wassmann, R., 2014. Common practices for manual greenhouse gas sampling in rice production: a literature study on sampling modalities of the closed chamber method. *Greenhouse Gas Measurement and Management* 4, 1–13. <https://doi.org/10.1080/20430779.2014.892807>
- Säurich, A., Tiemeyer, B., Dettmann, U., Fiedler, S., Don, A., 2021. Substrate quality of drained organic soils—Implications for carbon dioxide fluxes. *J. Plant Nutr. Soil Sci.* 184, 543–555. <https://doi.org/10.1002/jpln.202000475>
- SMHI, 2023. Data [WWW Document]. URL <https://www.smhi.se/data>
- Virtanen, P., Gommers, R., Oliphant, T.E., Haberland, M., Reddy, T., Cournapeau, D., Burovski, E., Peterson, P., Weckesser, W., Bright, J., van der Walt, S.J., Brett, M., Wilson, J., Millman, K.J., Mayorov, N., Nelson, A.R.J., Jones, E., Kern, R., Larson, E., Carey, C.J., Polat, İ., Feng, Y., Moore, E.W., VanderPlas, J., Laxalde, D., Perktold, J., Cimrman, R., Henriksen, I., Quintero, E.A., Harris, C.R., Archibald, A.M., Ribeiro, A.H., Pedregosa, F., van Mulbregt, P., SciPy 1.0 Contributors, Vijaykumar, A., Bardelli, A.P., Rothberg, A., Hilboll, A., Kloeckner, A., Scopatz, A., Lee, A., Rokem, A., Woods, C.N., Fulton, C., Masson, C., Häggström, C., Fitzgerald, C., Nicholson, D.A., Hagen, D.R., Pasechnik, D.V., Olivetti, E., Martin, E., Wieser, E., Silva, F., Lenders, F., Wilhelm, F., Young, G., Price, G.A., Ingold, G.-L., Allen, G.E., Lee, G.R., Audren, H., Probst, I., Dietrich, J.P., Silterra, J., Webber, J.T., Slavič, J., Nothman, J., Buchner, J., Kulick, J., Schönberger, J.L., de Miranda Cardoso, J.V., Reimer, J., Harrington, J., Rodríguez, J.L.C., Nunez-Iglesias, J., Kuczynski, J., Tritz, K., Thoma, M., Neville, M., Kühnmerer, M., Bolingbroke, M., Tartre, M., Pak, M., Smith, N.J., Nowaczyk, N., Shebanov, N., Pavlyk, O., Brodtkorb, P.A., Lee, P., McGibbon, R.T., Feldbauer, R., Lewis, S., Tygier, S., Sievert, S., Vigna, S.,

- Peterson, S., More, S., Pudlik, T., Oshima, T., Pingel, T.J., Robitaille, T.P., Spura, T., Jones, T.R., Cera, T., Leslie, T., Zito, T., Krauss, T., Upadhyay, U., Halchenko, Y.O., Vázquez-Baeza, Y., 2020. SciPy 1.0: fundamental algorithms for scientific computing in Python. *Nat Methods* 17, 261–272. <https://doi.org/10.1038/s41592-019-0686-2>
- Wagner, S.W., Reicosky, D.C., Alessi, R.S., 1997. Regression Models for Calculating Gas Fluxes Measured with a Closed Chamber. *Agronomy Journal* 89, 279–284. <https://doi.org/10.2134/agronj1997.00021962008900020021x>
- Worrall, F., Boothroyd, I.M., Gardner, R.L., Howden, N.J.K., Burt, T.P., Smith, R., Mitchell, L., Kohler, T., Gregg, R., 2019. The Impact of Peatland Restoration on Local Climate: Restoration of a Cool Humid Island. *J. Geophys. Res. Biogeosci.* 124, 1696–1713. <https://doi.org/10.1029/2019JG005156>
- WRB, 2015. World Reference Base for Soil Resources 2014, update 2015 International soil classification system for naming soils and creating legends for soil maps.
- Wutzler, T., Lucas-Moffat, A., Migliavacca, M., Knauer, J., Sickel, K., Šigut, L., Menzer, O., Reichstein, M., 2018. Basic and extensible post-processing of eddy covariance flux data with REddyProc. *Biogeosciences* 15, 5015–5030. <https://doi.org/10.5194/bg-15-5015-2018>
- Xu, J., Morris, P.J., Liu, J., Holden, J., 2018. PEATMAP: Refining estimates of global peatland distribution based on a meta-analysis. *CATENA* 160, 134–140. <https://doi.org/10.1016/j.catena.2017.09.010>
- Yu, Z., Beilman, D.W., Frolking, S., MacDonald, G.M., Roulet, N.T., Camill, P., Charman, D.J., 2011. Peatlands and Their Role in the Global Carbon Cycle. *EoS Transactions* 92, 97–98. <https://doi.org/10.1029/2011EO120001>

Popular science summary

Peatlands are a globally important carbon (C) store, holding about 21% of total soil C. In their natural state, most peatlands are sinks for atmospheric carbon dioxide (CO₂), but are sources of methane (CH₄) and small amounts of nitrous oxide (N₂O). Large areas of natural peatlands are drained for peat extraction, agriculture, or forestry. Drainage leads to oxidative peat decomposition, degrading organic material and leading to high CO₂ emissions. When peatlands are used for agriculture, the use of nitrogen fertiliser often leads to elevated N₂O emissions.

Under the EU Common Agricultural Policy, direct payments are offered to farms that set aside, *i.e.* leave fallow, agricultural land on drained peat, in order to reduce greenhouse gas (GHG) emissions. However, in the scientific literature, there is growing evidence that this may be an ineffective GHG mitigation strategy. To increase understanding on the effect of agricultural management intensity on GHG emissions from drained peatlands, in this thesis GHG fluxes from two adjacent fields (cropland and set-aside grassland) were measured over a period of more than six years. Two widely used measurement methods were employed, the eddy covariance (EC) method and the chamber method.

In addition, a relaxed eddy accumulation (REA) system that allows continuous flux measurements of CO₂, N₂O, CH₄, and water vapour from ecosystems was developed and tested. The chamber measurement technique was optimised in terms of measurement duration, sampling frequency, and analyser precision.

The results showed that the set-aside grassland was a greater source of CO₂, a smaller source of N₂O and a larger sink of CH₄ than the cultivated cropland. The N₂O and CH₄ fluxes had minor effects on the GHG balance on both sites. Thus, these results support recent claims that setting-aside

farmland on drained peat is likely not an effective way to reduce agricultural GHG emissions as long as the peatland remains in a drained state.

The REA system was found to be capable of reliably measuring continuous fluxes of CO₂, N₂O, CH₄, and water vapour during the growing season, and even in winter months, in the Nordic climate. Flux comparisons with an EC system that was run in parallel showed good agreement for CO₂ and water vapour fluxes measured with both systems. The calculated detection limits for N₂O and CH₄ fluxes and the good agreement with results from the EC system suggest that the REA system can be used for flux monitoring of all relevant GHGs above terrestrial ecosystems. Furthermore, the sampling system's modular design and low energy demands make the REA system useful for remote and off-grid applications.

Using the simple and convenient method developed in this thesis, individual chamber flux measurements of N₂O and CH₄ can now be optimised for measurement duration, concentration sampling frequency, and the analyser's detection limit.

In conclusion, this thesis sheds new light on the complex dynamics of GHG emissions from drained peatlands under different agricultural management practices. While setting-aside farmland on drained peat is currently considered a GHG mitigation strategy, the findings in this thesis question its effectiveness. Future, development and testing of advanced measurement technologies, such as the REA system, will improve the ability to capture continuous and accurate fluxes and contributes to the broader goal of robust GHG flux monitoring. This thesis makes a small but important contribution to the ongoing dialogue on mitigating climate change and preserving critical C stores within ecosystems. However, with rapidly progressing climate change, it is increasingly urgent to implement recommendations on which the scientific community has reached consensus. Knowledge exists on how to limit the severity of climate change; the world only needs brave politicians to take the bold steps required.

Populärvetenskaplig sammanfattning

Torvmarker utgör en globalt viktig sänka för kol (C) och står för cirka 21% av markens totala kollagring. I sitt naturliga tillstånd är de flesta torvmarker en sänka för atmosfärisk koldioxid (CO_2), och en källa för metan (CH_4) och små mängder lustgas (N_2O). Stora områden med naturliga torvmarker dräneras dock för torvutvinning, jordbruk eller skogsbruk. Dikning leder till oxidativ nedbrytning av torv, vilket bryter ned organiskt material och leder till stora CO_2 -utsläpp. När torvmarker används för jordbruk leder användningen av kvävegödsel ofta till förhöjda N_2O -utsläpp.

Inom ramen för EU:s gemensamma jordbrukspolitik erbjuds direktstöd till jordbrukare som lägger jordbruksmark på torvmark i träda för att minska utsläppen av växthusgaser (GHG) genom avsättningar. I den vetenskapliga litteraturen finns det dock allt fler belegg för att detta kan utgöra en ineffektiv strategi för minskade utsläpp. För att öka vår förståelse över effekten av jordbruksintensitet har på växthusgasutsläpp från dränerade torvmarker mätte vi växthusgasflöden från två intilliggande fält, en odlingsmark och en gräsmark som tagits ur bruk under en period på mer än sex år. För detta ändamål valdes två allmänt använda metoder: eddy kovarians (EC) samt kammarmetoden.

Vi utvecklade och testade dessutom ett eddy ackumulationssystem med lättade krav (relaxed eddy accumulation-system, REA) som möjliggjorde kontinuerliga flödesmätningar av CO_2 , N_2O , CH_4 och vattenånga från ekosystemen. Mätteknikerna i kammaren optimerades på grundval av mättid, provtagningsfrekvens och analysprecision.

Vi fann att den avsatta gräsmarken utgjorde en större källa till CO_2 , en mindre källa till N_2O , och en större sänka för CH_4 än den odlade åkermarken. N_2O - och CH_4 -flöden hade dock mindre effekter på platsernas globala uppvärmningspotential. Baserat på våra resultat och i överensstämmelse med

andra nyligen genomförda studier är det därför avsättningen av jordbruksmark på dränerad torv sannolikt inte ett effektivt sätt att minska jordbrukets utsläpp av växthusgaser, så länge torvmarken förblir dränerad.

REA-systemet kunde mäta kontinuerliga flöden av CO₂, N₂O, CH₄ och vattenånga under växtsäsongen men även under vintermånaderna i det nordiska klimatet. Flödesjämförelser med ett EC-system som kördes parallellt visade god överensstämmelse för flöden av CO₂- och vattenånga uppmätta med båda systemen. De beräknade detektionsgränserna för N₂O- och CH₄-flöden och den goda överensstämmelsen med EC-systemet tyder på att REA-systemet kan användas för flödesövervakning av växthusgaser över markytan i terrestra ekosystem. Dessutom gör provtagningsystemets modulära design och låga energibehov det användbart för fjärr- och off-grid-tillämpningar.

Med en enkel och praktisk metod som utvecklats i denna avhandling kan flödesmätningar av N₂O och CH₄ i enskilda kammare nu optimeras för mätlängd, frekvens för koncentrationsprovtagning och analysatorns detektionsgräns.

Sammanfattningsvis bidrar vår studie till att klargöra mer av den komplexa dynamiken kring växthusgasutsläpp från dränerade torvmarker under olika jordbrukshanteringsmetoder. Att avsätta jordbruksmark på dränerad torv har ansetts vara en potentiell strategi för att minska växthusgasutsläpp, men våra resultat ifrågasätter effektiviteten i detta tillvägagångssätt. Dessutom förbättrar utvecklingen och testningen av avancerad mätteknik, såsom REA-systemet, vår förmåga att uppmäta kontinuerliga och exakta flöden och bidrar till det bredare målet gällande robust övervakning av växthusgasflöden. Avhandling utgör således ett litet bidrag till pågående ansträngningar att mildra klimatförändringarna och att bevara kritiska C-förråd i ekosystem. Ju mer vårt klimat förändras, desto mer brådskande blir det dock att genomföra de rekommendationer forskarsamhället har nått konsensus om. Vi vet hur vi kan begränsa klimatförändringarna, nu krävs av modiga politiker att de tar de första djärva stegen på vägen.

Populärwissenschaftliche Zusammenfassung

Moore sind wichtige Kohlenstoffspeicher weltweit und speichern etwa 21% des gesamten Bodenkohlenstoffs. In ihrem natürlichen Zustand sind die meisten Moore Senken für atmosphärisches Kohlendioxid (CO_2) und Quellen für Methan (CH_4) sowie geringe Mengen an Lachgas (N_2O). Moore wurden großflächig für den Torfabbau, die Land- oder Forstwirtschaft entwässert. Die Entwässerung führt zur oxidativen Zersetzung des organischen Materials in Mooren, dem Torf, wodurch große Mengen an CO_2 freigesetzt werden. Unter landwirtschaftlicher Nutzung führt der Einsatz von Stickstoffdünger häufig zusätzlich zu erhöhten N_2O -Emissionen.

Im Rahmen der Gemeinsamen Agrarpolitik der EU werden landwirtschaftlichen Betrieben, die Ackerflächen auf entwässerten Mooren stilllegen, Direktzahlungen angeboten, mit dem Ziel, die Treibhausgasemissionen entwässerter Mooreböden zu reduzieren. In der wissenschaftlichen Literatur häufen sich jedoch die Hinweise darauf, dass dies eine ineffektive Strategie ist.

Um die Auswirkungen der landwirtschaftlichen Nutzungsintensität auf die Treibhausgasemissionen von entwässerten Mooren besser zu verstehen, haben wir die Treibhausgasflüsse von zwei benachbarten Feldern, einem Acker und einem stillgelegten Grünland, über einen Zeitraum von mehr als sechs Jahren gemessen. Hierfür wurden zwei verbreitete Methoden gewählt: die Eddy-Kovarianz- (EC) und die Kammermethode. Außerdem wurde ein Relaxed Eddy Accumulation-System (REA) entwickelt und getestet, das kontinuierliche Flussmessungen von CO_2 , N_2O , CH_4 und Wasserdampf über Ökosystemen ermöglicht. Die Kammermessmethodik wurde in Bezug auf Messdauer, Häufigkeit der Konzentrationsmessungen und unter Berücksichtigung der Präzision des Analysegeräts optimiert.

Im Rahmen dieser Arbeit fanden wir heraus, dass beide Standorte CO₂-Quellen darstellten. Jedoch emittierte das stillgelegte Grünland eine größere Menge an CO₂, als das Ackerland. Lachgas- und CH₄-Flüsse hatten einen geringen Einfluss auf die Klimabilanz beider Standorte. Basierend auf unseren Ergebnissen und in Übereinstimmung mit weiteren Studien ist die Stilllegung von Ackerland auf entwässertem Torf kein wirksames Mittel zur Verringerung der landwirtschaftlichen Treibhausgasemissionen, solange der Standort nicht wiedervernässt wird.

Das REA-System zeichnete kontinuierlich und verlässlich CO₂-, N₂O-, CH₄- und Wasserdampf Flüsse über mehrere Wachstumsperioden und sogar in den Wintermonaten des nordischen Klimas auf. Flussvergleiche mit einem parallel installierten EC-System zeigten eine gute Übereinstimmung der CO₂- und Wasserdampf Flüsse, und die berechneten Nachweisgrenzen für N₂O- und CH₄-Flüsse stimmten zuversichtlich, dass das REA-System für die Messung aller relevanten Treibhausgasflüsse von terrestrische Ökosysteme eingesetzt werden kann. Darüber hinaus ist das System aufgrund des modularen Aufbaus und des geringen Energiebedarfs auch für abgelegene und netzunabhängige Anwendungen geeignet.

Nach den Ergebnissen dieser Studie ist die Stilllegung von Ackerland auf entwässerten Mooren mit dem Ziel Treibhausgasemissionen zu reduzieren, ineffektiv bis kontraproduktiv. Somit ist ein Umdenken auf politischer Ebene dringend notwendig. Diese Studie trägt nicht nur zur Weiterentwicklung bestehender Messtechnologien bei, sondern ist auch ein Beitrag zum Diskurs über die Abschwächung des Klimawandels und den Erhalt wichtiger Kohlenstoffspeicher natürlicher Ökosystemen. Je weiter sich unser Klima verändert, desto dringlicher wird es, die Empfehlungen umzusetzen, über die die Wissenschaft längst einen Konsens erzielt hat. Wir wissen, wie wir das Ausmaß des Klimawandels begrenzen können; es braucht nur mutige Politiker, die die richtigen Schritte in die Wege leiten.

Acknowledgements

This thesis was carried out at the Ecology Department of the Swedish University of Agricultural Sciences (SLU) in Uppsala with financial support from the Swedish Farmers' Foundation for Agricultural Research (Stiftelsen Lantbruksforskning, contract no. O-18-23-169), the Faculty of Natural Resources and Agricultural Sciences (SLU), the Wallenberg Foundation, the Council of Postgraduate Education (SLU), and the International Peatland Society. Jan-Erik Olson and Sören Hedwall provided the study sites. I am grateful for all those contributions. Thanks also to the Department of Ecology and the research school Focus on Soils and Water for providing me with postgraduate education and relevant courses.

Many thanks are due to my supervisors! *Achim Grelle* for hiring me, providing the funding and giving me the freedom to develop my independence. *Katharina Meurer* for all the support in the field, with writing, and for the many good discussions, but particularly for your contagious joyful positivity topped with a generous use of sarcasm that helped cheering me up on countless occasions! Thank you *Sabine Jordan* for showing me the beauty of peatlands, inspiring my projects and supporting me with equipment, in the field, and the writing process. Thank you *Thomas Kätterer* for discussing the project, giving valuable input, reliably replying to emails, patiently answering my questions, and having a listening ear for the challenges I encountered on the way.

But most importantly I would like to thank all my supervisors for letting me go adventuring on the most remote place on earth and for welcoming me back thereafter!

Further, I want to thank *Chis Evans*, *Ross Morrison*, and *Alex Cumming*, for the time at UKCEH, the fun fieldwork days on the peatlands of Southern England, and for the discussions on measurement techniques and EC data

analysis. Thanks to *Gustav Granath* for the kind support during fieldwork and student supervision. Many thanks to *Jan Fiedler* for all the joyfully productive discussions on measurement techniques, detection limits, and chamber design and for your selfless support to any hour of the day. Thank you *Astrid Taylor*, I very much appreciated your support during times of troubled waters. Thank you *John Köstel* for supporting various small side projects, besides always being there for a good laugh! I also thank the *System Ecology* group for the Monday fika meetings and the suggestions and support that came up during those. I further appreciated the valuable comments and suggestions from the *Anonymous Reviewers* that helped improve the papers of this thesis. Thank you *Tord* for lifting my Swedish poetry to a completely new level and thanks to *Mary* for doing the same to my English. And for the help during fieldwork from *Gloria, Arthee, and Bernabé* am very grateful.

I am grateful to *Vincent Felde*, if it wasn't for him I would have likely chosen a different path.

Big thanks go to the members of the overwintering team 42 at Neumayer III Station. Thank you *Alicia, Aurelia, Benita, Karsten, Katrin, Markus, Micha, and Werner* for a beautiful year on-ice full of excitement and by that helping me regain the necessary motivation to finish this thesis!

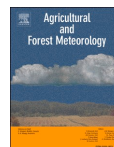
And Thanks to past and present PhD students, Post-Docs and friends for making work more fun and social live a highlight, especially *Alex, Anna, Ben, Björn, Caitlin, Chloë, Dimitrije, Dragos, Eirini, Fabiola, Gloria, Guillermo, Ineta, Janina, Julian, Juliana, Kate, Kirstin, Laura, Lorenzo, Marcos, Max, Merlin, Ortrud, Pierre, Rafaele, Renee, Sepp, Tord, Yuval, et al.* And thanks to the whole lot of current PhD students and Post-Docs for warmly welcoming me back and for all the cake, the cookies and biscuits during fika breaks!

Und lieben Dank an meine Eltern, Gisela und Bernd für Euer Verständnis für meinen Lebensstil als Wissenschaftsvagabund.



Contents lists available at ScienceDirect

Agricultural and Forest Meteorology

journal homepage: www.elsevier.com/locate/agrformetAffordable relaxed eddy accumulation system to measure fluxes of H₂O, CO₂, CH₄ and N₂O from ecosystemsAchim Grelle^{*}, Hannes Keck

Department of Ecology, Swedish University of Agricultural Sciences, Uppsala, Sweden

ARTICLE INFO

Keywords:

REA
Micrometeorology
Conditional sampling
Greenhouse gas fluxes
Turbulent fluxes
Nitrous oxide

ABSTRACT

The relaxed eddy accumulation (REA) technique is frequently applied to measure fluxes of a large variety of atmospheric tracers above ecosystems. It is often the method of choice since the eddy covariance (EC) technique is limited to a few tracers due to the lack of fast response analysers, high financial costs and in some cases high power consumption. REA avoids the need for a fast response analyser by collecting air from up-drafts and down-drafts into separate reservoirs. After collecting the air over a predefined time period, trace gas concentrations in the reservoirs are analysed by a slow response analyser and the average fluxes can be calculated.

We developed and tested a REA system that is capable of measuring CO₂, CH₄, N₂O and H₂O fluxes simultaneously with only one gas analyser (Picarro G2805). This system is compatible with virtually any gas analyser and thus supports the flux analysis of a wide range of other air constituents such as isotopes, aerosols and volatile organic compounds. Furthermore, the modular design and rugged casing makes the sampling system robust and portable, and with its 12 V DC operation it is suitable for a wide range of field campaigns. The performance of the REA system was tested during the growing seasons of 2018 and 2020 on a grassland on organic soil in central Sweden.

The system has worked reliably during several months in the Nordic climate, covering ambient temperatures between -20°C and +30°C. Measured fluxes of CO₂ and H₂O agree well with fluxes measured independently by an EC system. The similarity in the technology and the determined detection limits made us confident that the REA system even captures fluxes of CH₄ and N₂O well.

1. Introduction

Micrometeorological methods are gaining in importance for trace gas flux measurements above terrestrial ecosystems (e.g. [Bugster and Merbold, 2015](#)). These methods enable measurements of average gas fluxes from a large area over extended time periods and with a high temporal resolution by sampling the turbulent gas exchange in the atmospheric boundary layer. Most widely used, the eddy covariance (EC) method provides measurements of gas fluxes between ecosystems and the atmosphere with a typical representative source area (or “flux footprint”) of several hectares. It builds upon simultaneous sampling of turbulent wind components and gas concentrations at typical sampling rates of 10–20 Hz. But it is still limited to a small number of gas species due to the lack of fast-response gas analysers and low signal-to-noise ratios. Furthermore, its applicability for small atmospheric constituents such as nitrous oxide is often limited by high power consumption.

Eddy accumulation represents an alternative system for turbulent

exchange measurements that continuously collects air from instant up- and down-drafts into two separate reservoirs (or accumulates air constituents on denuders). After the sampling period (e.g., 30 minutes) the difference of gas concentrations between the updraft- and the downdraft-reservoirs are analysed with a gas analyser. Here, a high frequency response of the analyser is not required. The difference in gas concentration between the two reservoirs is related to the mean flux during the sampling period ([Desjardins, 1972](#)). For this so called “true” eddy accumulation technique the air flow into the reservoirs must be proportional to the vertical wind velocity, which is technically demanding. [Businger and Oncley \(1990\)](#) relaxed the requirement of the airflow to be proportional to the vertical wind speed and proposed a “relaxed” version of eddy accumulation (Relaxed Eddy Accumulation, REA) that uses a constant flow rate.

The development of cavity ringdown spectroscopic (CRDS) analysers during recent years has made concentration measurements of small atmospheric constituents feasible and affordable, and has opened

^{*} Corresponding author.

E-mail address: achim.grelle@slu.se (A. Grelle).

<https://doi.org/10.1016/j.agrformet.2021.108514>

Received 12 March 2021; Received in revised form 25 May 2021; Accepted 7 June 2021

Available online 26 June 2021

0168-1923/© 2021 The Author(s). Published by Elsevier B.V. This is an open access article under the CC BY license (<http://creativecommons.org/licenses/by/4.0/>).

opportunities for gas flux measurements by the REA technique in particular. While the gas analysis is relatively easy to achieve by slow-response analysers, the technological challenge is to develop an exact, reliable, and durable fast-response air sampling system that collects updraft and downdraft air separately at a switching frequency of typically 10-20 Hz to capture the relevant ranges of the boundary layer turbulence spectrum.

Using a REA system, fluxes of a wide range of tracers such as carbon dioxide, nitrous oxide, methane, isotopes, aerosols, pollutants or volatile organic compounds have been measured occasionally (e.g., Beverland et al., 1996; Desjardins et al., 2010; Gaman et al., 2004; Haapanala et al., 2006; Hargreaves et al., 1996; Pattey et al., 2007; Ren et al., 2011; Osterwalder et al., 2016; Riederer et al., 2014).

Desjardins et al. (2010) and Pattey et al. (2007) used an aircraft-based REA system for campaigns to measure N₂O emissions close to Ottawa and Saskatoon, Canada. Beverland et al. (1996) measured CH₄ and N₂O fluxes and Hargreaves et al. (1996) measured N₂O fluxes by a REA system during periods of up to ten days. However, the REA technique has not yet been used to measure nitrous oxide, methane, carbon dioxide and water vapour fluxes simultaneously. Neither has it been used to measure fluxes over complete agricultural seasons. To estimate regional nitrous oxide emissions reliably it is of great importance to monitor fluxes corresponding to complete agricultural seasons and large geographical areas (field scale and above). Principally, both conventional EC and REA systems can provide this type of data. However, the implementation of EC systems for minor atmospheric constituents bears a high initial cost and high power consumption, and also transportation to remote places and powering the systems at site can be difficult. Furthermore, for measuring all relevant GHG fluxes from a terrestrial ecosystem using an EC system there is no single fast-response gas analyser currently available. Whereas, for a REA system a cavity ringdown gas spectrometer (e.g., Picarro G2508) can be used to analyse water vapour, methane, carbon dioxide and nitrous oxide simultaneously.

Here, we present a new REA system that basically consists of commercially available standard components, which makes it affordable. It is capable of measuring CO₂, N₂O, CH₄ and water vapour fluxes reliably over complete growing seasons, and we critically evaluate its performance during the growing seasons of 2018 and 2020.

2. Material and methods

2.1. Theory

The concentration difference between updraft and downdraft reservoirs ($C_{up} - C_{down}$) is related to the mean flux F by

$$F = \beta \cdot \sigma_w \cdot (C_{up} - C_{down}) \tag{1}$$

Where σ_w is the standard deviation of the vertical wind speed, determined by a sonic anemometer operating at 10 Hz, and β is an empirical coefficient with a value of about 0.6 (Businger and Oncley, 1990). In this study, we determined β by relating the sensible heat flux, estimated by eddy-covariance (H_{EC}) to the sensible heat flux, estimated by REA (H_{REA}).

$$H_{EC} = \rho \cdot c_p \cdot \overline{wT'}$$

$$H_{REA} = \rho \cdot c_p \cdot \beta \cdot \sigma_w \cdot (T_{up} - T_{down}) \tag{2}$$

where ρ = air density, c_p = specific heat at constant pressure, $\overline{wT'}$ = covariance of vertical wind velocity and air temperature. Setting $H_{REA} = H_{EC}$ the parameter β becomes

$$\beta = \frac{\overline{wT'}}{\sigma_w (T_{up} - T_{down})} \tag{3}$$

Based on 5 months of measurements over an agricultural field the

coefficient on average thus evaluated to $\beta = 0.475 \pm 0.29$ (standard deviation).

Air is sampled into the corresponding reservoir depending on the direction of the vertical wind velocity w (conditional sampling), but only if the vertical wind speed exceeds a certain threshold value, the dead-band velocity w_0 . Given the limited resolution and accuracy of the sonic anemometer, a choice of $w_0 = 0$ would result in considerable amounts of air erroneously sampled in either of the reservoirs during periods when the vertical wind velocity is practically zero. Choosing a large dead-band, on the other hand, would favour conditions of high vertical wind speed and imply larger numbers of individual air samples during well-mixed periods at daytime than during calm periods at night. Obviously, a dynamic dead-band should be used to adapt the sampling setup to the turbulence conditions such that similar amounts of air are sampled during all times of the day.

In this study we chose σ_w as a practical measure for turbulent mixing that determines the dead-band w_0 . To test the impact of w_0 on the sampling system we monitored the duration of opening for each valve. Empirically we found that

$$w_0 = \frac{\sigma_w}{3.5} \tag{4}$$

was a suitable relation that yielded similar amounts of air in the updraft and downdraft reservoirs, respectively, and reasonable numbers of individual samples during both day and night. In practice, out of 18000 samples during a sampling interval ca. 4000 samples were within the dead-band (implying closed valves) during daytime, whereas ca. 8000 samples corresponded to the dead-band during night on average. A larger share of dead-band conditions during night is natural because of lower turbulent mixing Table 1.

While the REA fluxes scale linearly with β , their dependence on w_0 is less straightforward. Near a surface, strong fluctuations in vertical velocity are associated with strong fluctuations in horizontal velocity, and are caused by large, coherent eddies (e.g., Katul et al., 2006). That implies that the use of a dead-band favours the sampling of larger eddies, which shifts the sampled turbulence spectrum towards lower frequencies. But in contrast to a limited high-frequency response that may be inherent in an EC system, this does not cut off all high-frequency signals, but only excludes samples with very small vertical displacement that hardly contribute to the fluxes. Furthermore, the dead-band may lead to an increase of concentration differences between the reservoirs (e.g., Tsai et al., 2012). One reason for that is that a higher fraction of air samples with larger vertical displacement is collected. This is however moderated to some extent because the occurrence of large eddies in the boundary layer is usually associated with smaller vertical concentration gradients. In principle, that corresponding increase in ($C_{up} - C_{down}$) should be compensated by a decrease in β (e.g., Bowling et al., 1999). Another reason for the increase is that dilution of air in the reservoirs by samples with zero or opposite vertical displacement is avoided, which is necessary for accurate measurements.

In fact, an increasing dead-band increases the magnitude of the measured fluxes. Fig. 1 shows REA-CO₂ fluxes simulated from EC data with dead-bands ranging from zero to $2w_0$ from Eq. (4), with a constant $\beta = 0.475$. While doubling or removing the dead-band can affect

Table 1
Feature comparison between REA and EC systems.

Feature	REA	EC
Frequency response	Limited by sonic anemometer	Limited by sonic anemometer, gas analyser, and air transport system
Algorithm	Individual eddies are dampened	Individual eddies are captured
Sensor misalignment	Handled by high-pass filter	Handled by coordinate rotation
Sloping terrain	Handled by high-pass filter	Handled by coordinate rotation

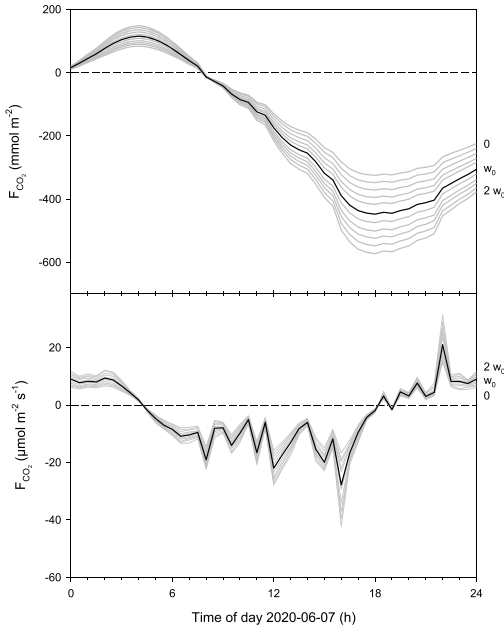


Fig. 1. The influence of w_0 on REA- CO_2 fluxes, simulated from EC-rawdata with $\beta = 0.475$. The black lines denote a dead-band of w_0 used in this study, the grey lines denote changes of the dead-band in 20% steps, ranging from zero to $2 w_0$. Upper graph: cumulative fluxes; lower graph: half-hourly fluxes.

individual fluxes by up to 30%, changes of the dead-band by, say, 10% have only marginal impact on the fluxes (Fig. 1).

A dynamic dead-band that is adapted to actual turbulence conditions as described above assures adequate sampling and accurate concentration differences. Using this dynamic dead-band, our β did not show any seasonality or consistent diurnal dynamics and can therefore be assumed constant, in agreement with Haapanala et al. (2006) and Grönholm et al. (2008).

It is difficult to clearly identify variables that affect the determination of w_0 and β , and it is recommended for each field application to investigate the values in order to check the validity of the parameterisation or to detect measurement problems (Ammann and Meixner, 2002).

2.2. System setup

The main components of the REA system are a 3D ultrasonic anemometer (Solent 1012R3, Gill Instruments, Lymington, UK), 2 identical pairs of sample air reservoirs (12 L Tedlar bags, SKC 232-10, Eighty Four, PA, USA), a G2805 CRDS analyser (Picarro inc., Santa Clara, CA, USA) and a CR1000 Measurement and Control Datalogger (Campbell Scientific, Logan, UT, USA). 2 pairs of sample reservoirs are needed to provide continuous measurements: while one pair of reservoirs is used to collect air samples, the other pair can be analysed.

Sample air is taken in below the anemometer's measuring volume (distance ca. 15 cm) and lead to the reservoirs through parallel Teflon tubes (ScanTube, diameter $\frac{1}{8}$ ""). To avoid contamination, an SLFA05010 PTFE filter is installed in each tube close to the inlet (1 μm , Merck Millipore, Darmstadt, Germany). Using two independent tubes avoids mixing of updraft- and downdraft air, and thus no turbulent air flow in

the tubes is required (Bowling et al., 1998). Opening and closing of the respective reservoir is achieved by fast-switching stainless-steel solenoid valves (6011, Buerkert, Ingelfingen, Germany) controlled by the datalogger via an SDM-CD16AC relay driver (Campbell Scientific, Logan, UT, USA). To achieve a constant flow rate of 0.8 L min^{-1} through the sampling tubes and to avoid sample contamination, the sampled air does not pass any pump. Instead, each pair of Tedlar bags is placed in a common sealed IM2720 container (Pelican Products Inc., Torrance, CA, USA) that is partly evacuated by means of a 1420VDP air pump (Gardner Denver Thomas GmbH, Fürstfeldbruck, Germany). The pressure difference between the container and the atmosphere is measured by a 100KPDW differential pressure sensor (Fujikaru Ltd., Tokyo, Japan) and is kept constant at ca. 20 hPa by control of the datalogger. This principle that reminds of "ballonets" used in airships ensures both filling of the Tedlar bags when under-pressure is applied, and emptying of the bags when over-pressure is applied. The corresponding air flows are directed by means of 3-way stainless-steel solenoid valves (30334, Rotex, Maharashtra, India). During analysis of the reservoir content, air is drawn from the Tedlar bags via another SLFA05010 filter and through the G2508 CRDS analyser by an A0702 closed System pump (Picarro inc., Santa Clara, CA, USA). The G2508 reports gas concentrations in dry mole fractions, which means that no correction for density fluctuations due to latent heat fluxes (e.g., Bowling et al., 1998) is necessary. Concentration data are transferred to the datalogger by RS232 communication. The principle setup of the REA system is shown in Fig. 2.

The G2508 analyser and the A0702 pump are powered by 230 VAC; the rest of the system is powered by 12 VDC. Together with the modular construction this provides mobility and flexibility, since virtually any gas analyser or even several analysers in a sequence can easily be connected to the system. The G2508 and the CR1000 datalogger are connected to the internet by a wireless router for remote control and data retrieval.

The system is placed in an insulated, heated, and ventilated trailer to maintain appropriate operating conditions. Diodes are installed to protect the SDM-CD16AC against voltage kickback when switching inductive loads such as solenoids. System temperature is monitored by a thermocouple that enables the logger to switch off the system in case of overheating. Power supply is secured by residual current devices, fuses and transient protection.

2.3. Principle of operation

Initially both pairs of sample reservoirs are exposed to under-pressure. The sonic anemometer measures the turbulent wind components and the speed of sound at 10 Hz. A digital recursive low-pass filter (time constant = 200 s) is used for de-trending. If the remaining high-pass signals exceed the actual dead-band they are used to control the fast-switching solenoid valves. While the under-pressure in the containers is kept constant by control of the datalogger, the updraft- and downdraft reservoirs in the first container are successively filled with sample air through the fast-switching valves. After a sampling period of typically 30 minutes (larger reservoirs would be needed for longer periods) the sample air flow is directed into the second pair of reservoirs, while the first container is set to over-pressure.

While the second pair of reservoirs is filled by sample air in the same manner as the first, the collected air from the reservoirs in the pressurised container is led through the G2508 CRDS analyser. Each reservoir is analysed for 5 minutes at a sampling rate of 1 Hz. Prior to each analysis cycle a certain number of samples is skipped to avoid analysis of mixed air in the tubing. After 10 minutes the reservoirs are emptied completely and are thus ready for the next sampling period. Now the G2508 is free for 20 minutes to be used for other applications such as chamber- or profile measurements.

Raw data, processed fluxes and averages are stored on a CF memory card in the datalogger.

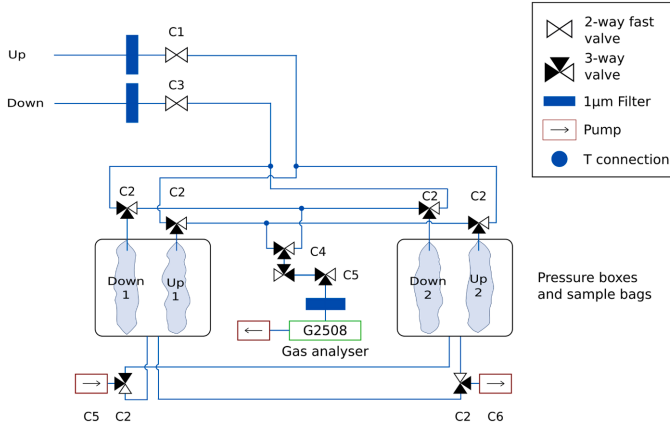


Fig. 2. Principle sketch of the REA system. C1 - C6 depict the control ports of the SDM-CD16AC relay driver.

2.4. Detection limit

We determined the analyser's standard deviations (SD) per gas by injecting a standardised gas sample (339 ppbv N₂O, 1.96 ppmv CH₄, 417.2 ppmv CO₂ and 0.55 % H₂O) over a period of 90 minutes. For each gas, the SD was calculated over the analysing period, except for H₂O (15 minutes) to minimize the risk of condensation. The standard deviations were found to be 3.81 ppbv, 0.37 ppbv, 0.15 ppmv, and 24 ppmv for

N₂O, CH₄, CO₂, and H₂O, respectively (n = 6750, n_{H2O} = 1125). Note that the determined SDs are considerably lower than the guaranteed precisions provided by the manufacturer. The REA system's detection limit (DL) was then calculated based on these SDs and a Monte Carlo analysis, similar to the approach of Parkin et al. (2012). We simulated 10⁴ times normal distributed gas concentrations over a measurement period of 5 minutes for both, the up-draft and the down-draft reservoir. The *norm* function of R (version 3.6.3; R Core Team, 2020) was used to

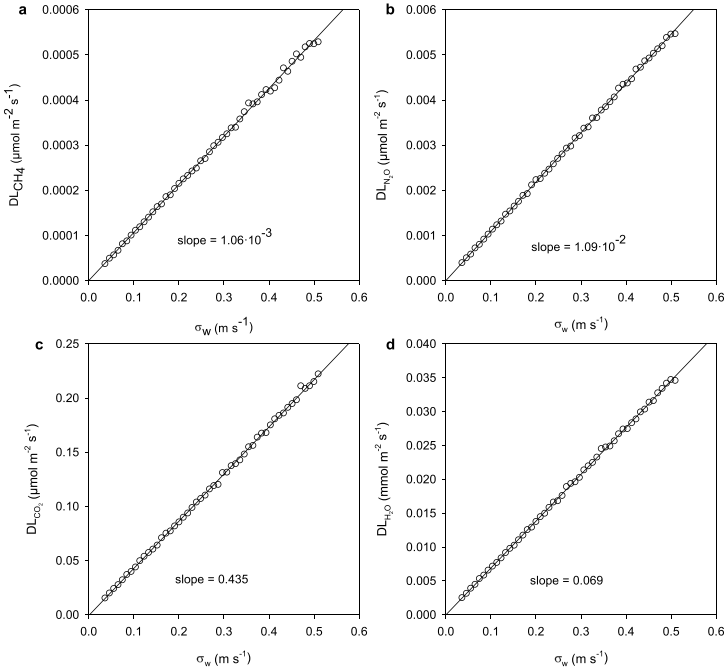


Fig. 3. Detection limits (DL) for gas fluxes as a function of the standard deviation of vertical wind speed as determined by Monte Carlo simulation.

simulate this data by providing it with the gas concentrations of the standardised air sample as mean parameters and the previously determined analyser's SDs as standard deviation parameters. This way we simulated zero-flux conditions. Using Eq. (1) with $\beta = 0.475$ and the simulated data as mean up-draft and down-draft concentrations the flux was calculated 10^4 times for a typical range of σ_w ($0.036 < \sigma_w < 0.5$). The detection limit was then defined as the respective 97.5 % percentile (Fig. 3). Since the detection limit for each gas scales linearly with σ_w specific values can be calculated by using the slope of the respective regression line in Fig. 3 as scale parameter. The detection limits for an average σ_w of 0.273 m s^{-1} are thereby $DL_{N_2O} = 2.98 \text{ nmol m}^{-2} \text{ s}^{-1}$, $DL_{CH_4} = 0.299 \text{ nmol m}^{-2} \text{ s}^{-1}$, $DL_{CO_2} = 0.119 \text{ } \mu\text{mol m}^{-2} \text{ s}^{-1}$, and $DL_{H_2O} = 0.019 \text{ mmol m}^{-2} \text{ s}^{-1}$.

3. Results

As a first test application, the REA system was deployed at a set-aside agricultural field site on drained peatland close to Harbo, Sweden ($60^\circ 5' \text{ N}$, $17^\circ 13' \text{ E}$). A more detailed site description is found in Hadden and Grelle (2017).

In parallel with the REA measurements, the sonic anemometer was even used for eddy-covariance measurements of CO_2 fluxes in combination with an LI6262 infrared gas analyser (LI-COR inc., Lincoln, NE, USA). Except for some gaps due to power failures, the REA system was continuously running from May to November 2018 and from July 2019 to May 2021 (currently ongoing).

A certain engineering challenge was the sealing of the pressurised containers. Incomplete sealing resulted in frequent starts of the air pumps to compensate for pressure drops (Fig. 4). This was less prominent for under-pressure, since the folding lock was pressed against the gasket by atmospheric pressure under those conditions. Here, mainly natural pressure drops due to the inflow of sample air into the reservoirs caused the pump to start frequently.

Two pronounced drops of the over-pressure after 10 minutes in each cycle (indicated by arrows) depict emptying of the two reservoirs after analysis. The pressure drops are reflected in changes in pumping frequency associated with longer filling periods. Occasional over- or undershooting of the target pressure occurs when the low-priority unit for pressure control in the datalogger program is ignored in favour of high-priority routines such as switching the fast valves.

The measured CO_2 mole fractions are mainly representative for ambient air within the ventilated trailer that houses the gas analyser, except during the analysis cycles (the first one starting at 900 seconds in Fig. 5). These are characterised by two plateaus representing the mole fractions in the two respective reservoirs. Here, the first plateau corresponds to a 5-minutes long analysis of the downdraft reservoir, the second one represents the updraft reservoir. A higher mole fraction in

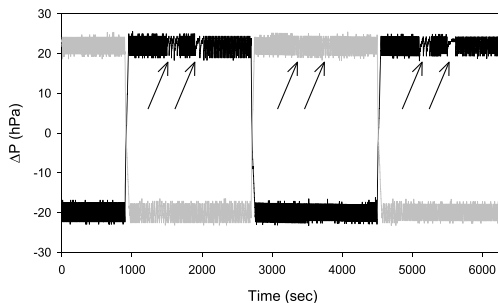


Fig. 4. Differential pressure in containers, 2018-07-11, 04:45 – 06:30. Black line corresponds to container 1, grey line to container 2. The arrows indicate the period when the sample reservoirs were emptied after analysis.

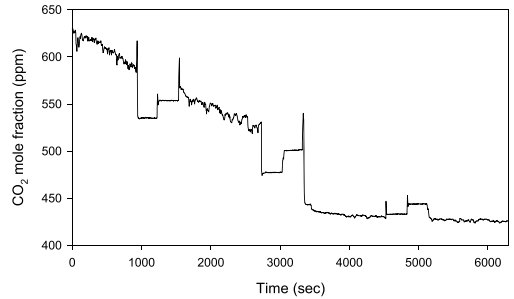


Fig. 5. CO_2 mole fractions 2018-07-11, 04:45 – 06:30. The first plateau in each sequence corresponds to downdraft analysis, the second to updraft analysis.

the updraft reservoir means an upward flux of CO_2 , i.e., a CO_2 emission from the ecosystem. During transitions from high to low CO_2 concentrations such as in Fig. 5, occasional spikes occur at the beginning or the end of such plateaus due to remaining air in the tubing that still holds the gas concentrations from the last analysis 30 minutes earlier. These samples are disregarded in the analysis, i.e., a programmable number of samples are automatically skipped after each switch of the analysis-valves. This course of concentrations is rather typical for an early morning after a calm night with stable stratification. A relatively large vertical gradient of CO_2 concentrations has built up during the night (the "storage term"), and the REA fluxes are characterized by small σ_w (low turbulent mixing) and large concentration differences ($C_{\text{up}} - C_{\text{down}}$). During the morning hours, the concentration gradient degrades (the storage term gets negative) through increasing turbulent mixing and eventually through photosynthesis, which is reflected in decreasing concentrations at measurement height and upward CO_2 fluxes.

A dynamic dead-band turned out to be necessary to provide reasonable numbers for down- and upward sampling under all atmospheric conditions. A static dead-band would systematically lead to larger numbers of daytime samples and an underrepresentation of nighttime samples, which in turn might lead to an underestimation of nighttime fluxes. A dynamic choice of a dead-band $w_0 = \sigma_w / 3.5$ corresponded to values between 0.01 m s^{-1} and 0.1 m s^{-1} , which resulted in ca. 14000 samples during day and 10000 samples during night ($n_{\text{up}} + n_{\text{down}}$, Fig. 6). This corresponds to 78% and 56% of the total number of samples during day and night, respectively. Occasionally (1.1% of cases) the number of samples dropped below 4000 per reservoir during stable night-time conditions when vertical wind speeds were very low.

3.1. Comparison between REA and EC

During periods of parallel measurements with both systems, a comparison of the resulting fluxes of CO_2 and H_2O was done. During 2018, no EC fluxes of H_2O were available. Therefore, a later period during 2020 was chosen, when an LI-7500 open path gas analyser (LI-COR inc., Lincoln, NE, USA) was available.

The half-hourly fluxes have been corrected for gas storage in the air column below the sensor, determined by differential changes of gas concentrations at sensor height. Since no concentration gradient below the sensor height is taken into account, this estimate represents a lower envelope of the true storage term, in particular for CO_2 where the surface is a net source during night. Since the gas-analyser is used in time-sharing mode, a multi-level system for vertical concentration profile measurements could be added to the REA system, which will be implemented in future versions.

No data screening concerning low turbulence conditions was applied ("ustar-filtering", cf. Aubinet et al., 2000), because system performance was to be evaluated rather than greenhouse gas budgets.

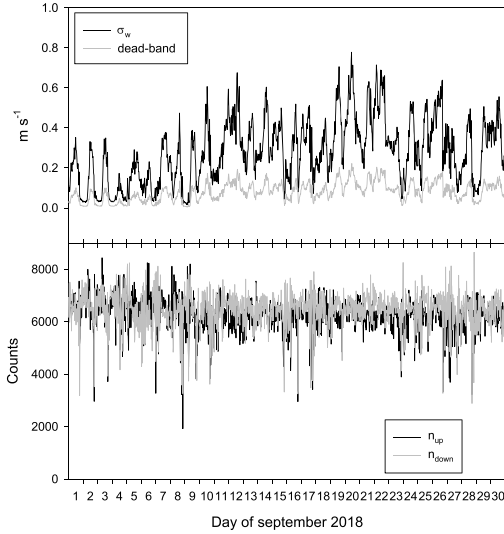


Fig. 6. Standard deviation σ_w of the vertical wind speed and corresponding dead-band (upper graph), and the resulting counts of open valve situations for sampling of downward (n_{down}) and upward (n_{up}) air parcels (lower graph).

Generally, the fluxes show a similar pattern that reflects the growing season dynamics of the site (Fig. 7). During the period between June and August 2018 the CO₂ budget of the site happened to be close to zero, with distinct sink- and source periods. For a budget comparison we chose the longest sink period (22/6 – 8/7) from which we determined an uptake of 135 g CO₂ m⁻² (EC) and 128 g CO₂ m⁻² (REA) by non-gapfilled data. There is a tendency towards higher uptake measured by the EC system during a period of small fluxes, i.e., a drought period in the middle of July. This was one of the warmest periods of the year, and the temperature surrounding the CRDS gas analyser occasionally exceeded the documented operational range (10°C – 35°C).

Larger emissions from the REA system can also be seen in the scatter plot (Fig. 8), along with a number of cases with relatively large fluxes from one system, while fluxes from the other system were close to zero. The discrepancies between zero fluxes from one system and large fluxes

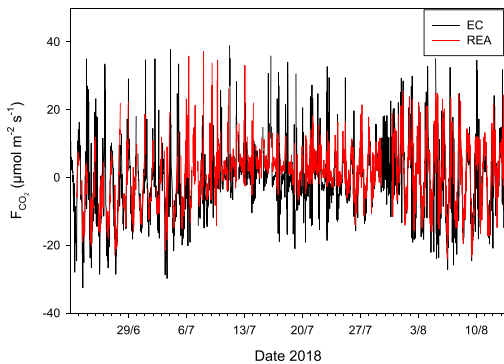


Fig. 7. CO₂ fluxes measured by EC (black line) and REA (red line) during summer 2018.

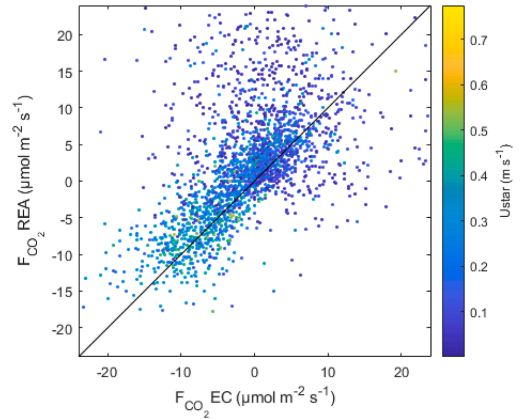


Fig. 8. CO₂ fluxes measured by REA versus fluxes measured by EC during summer 2018; the colour gradient depicts turbulent mixing.

from the other probably represent the challenge of measuring fluxes during stable atmospheric stratification and low turbulence intensity. At times, the EC system is not able to capture small-scale turbulence because of limited frequency response of the gas analyser, while the frequency response of the REA system is only limited by the frequency response of the sonic anemometer. On the other hand, cases of high EC flux and low REA flux may occur when single eddies contribute strongly to the covariance $w'CO_2'$, while their impact on the flux is dampened in the REA system by disregarding actual w' -components and using σ_w to represent vertical mixing. During these conditions, agreement between the EC system and a “true” relaxed eddy accumulation system would probably be better. However, a ustar-filtering (cf. Aubinet et al., 2000), as often done when gas budgets are to be determined, would effectively eliminate those conditions.

Even the water vapor fluxes were measured similarly by both systems (Fig. 9). Occasional lower EC fluxes than REA fluxes may be caused by a limited frequency response of the EC system, while occasional lower REA fluxes may reflect disregarding of individual w' samples, cf above. During the period 18/4 to 10/5 the total measured evapotranspiration from the site was 21.6 mm (EC) and 19.0 mm (REA) according to non-

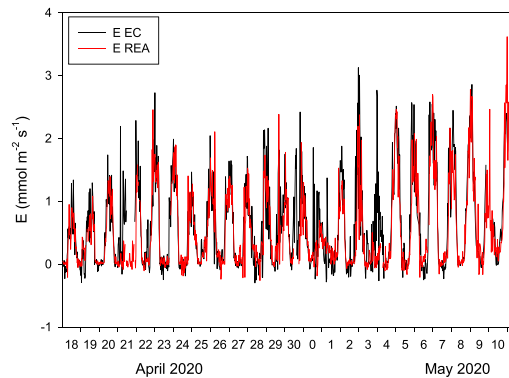


Fig. 9. H₂O fluxes measured by EC (black line) and REA (red line) during spring 2020.

gapfilled data.

In the scatter plot (Fig. 10) there appears to be a non-linear relationship between the two systems, with a trend towards a higher sensitivity of the REA system than the EC system during high evaporation conditions. Single points may be related to fluxes measured after a precipitation event, when the surfaces of the open path analyser had not dried completely yet, but were dry enough to produce data that passed the spike detection.

Data from both systems indicate occasional negative H₂O fluxes, which may be natural during dew formation.

4. Discussion

4.1. System calibration

Similar to EC systems, the fluxes measured by the REA system are directly proportional to the sensitivity (span) of the gas analyser, which has to be calibrated. The absolute gas concentration, or offset, is of minor importance, though it is preferable to be measured properly. In addition to the analyser calibration, the REA fluxes depend on the parameter β and the dead-band w_0 . The number of updraft and downdraft samples, as used in this study, is a suitable measure to determine the dead-band. This, in turn, affects β that can be determined by relating $\overline{T_{up} - T_{down}} / \overline{wT}$ (Eq. (3)). As long as a three-axis anemometer is used that provides data for speed-of-sound or air temperature, all required data are available in the REA system and no external measurements are required for calibration. Our choice of dead-band, $\sigma_w/3.5$, is smaller than $\sigma_w/2$ as proposed by Grönholm et al. (2008), and accordingly our $\beta = 0.475$ is slightly larger than Grönholm's $\beta = 0.42$.

Since no distinct seasonal or diurnal dynamics of β were observed, we conclude that no dynamic determination of β or any parameter recalibration is required, in agreement with Grönholm et al. (2008). In this way, we also avoided a possible bias in gas fluxes introduced by a dynamic β when the temperature difference ($T_{up} - T_{down}$) is small, and thus the denominator in Eq. (3) approaches zero (e.g., Grönholm et al. 2008).

4.2. Coordinate systems

Results from our comparison indicate that the REA system generally is capable to measure turbulent fluxes of CO₂ and H₂O with similar performance as the EC system. Occasional deviations between the two

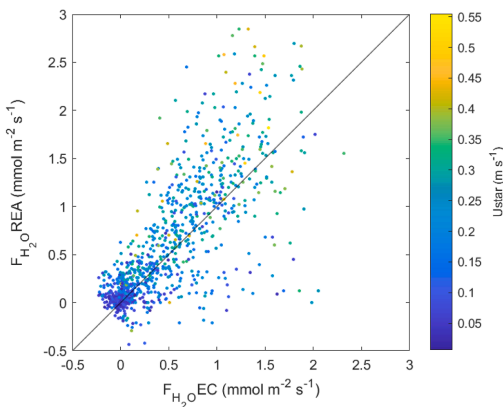


Fig. 10. H₂O fluxes measured by REA versus fluxes measured by EC during spring 2020; the colour gradient depicts turbulent mixing.

systems can partly be explained by technical differences that favour one or the other measurement system (Table 1).

A major difference between the two technologies is that post-processing of raw data can be done with an EC system, while it is impossible with a REA system: here, the raw turbulence data determine the switching of the fast valves and control the air flow, which cannot be altered in retrospect. In particular, coordinate rotations that correct for sensor misalignment and complex terrain (Aubinet et al., 2000) rely on available data prior to the rotation, either on a half-hourly (mean wind vector) or long-term (terrain topography) basis.

A REA system switches the valves depending on the vertical wind component that may be affected by sensor misalignment and terrain topography. In particular under conditions of strong lateral wind, when the direction of the measured vertical wind component is especially sensitive to sensor misalignment, this implies that errors may occur when air is sampled in the wrong reservoir.

High-pass filtering of the vertical wind component w reduces effects of misalignment and topography and yields fluxes perpendicular to the mean wind vector defined by the filter time constant. Especially with relatively small filter time constants, however, that mean wind vector may vary during the average time. Otherwise, for a REA system this filtering is more or less equivalent to a coordinate rotation, since the magnitude of w does not affect the fluxes directly, but only through the dead band w_0 when w is small. However, in an analysis of different filter techniques Bowling et al. (1998) concluded that the effects are surprisingly small and that none of the studied methods “provided better results than simply using raw, biased wind data to segregate updrafts and downdrafts”.

An EC system, on the other hand, can estimate fluxes perpendicular to the current mean wind vector determined during the average time, or perpendicular to the average earth surface, defined by a surface parameterisation or a long-term average of measured wind vectors.

A method to use the same coordinate system for both REA and EC fluxes could be a real-time coordinate transformation of the instantaneous wind vector. For this, a lookup-table of inclination angles as a function of wind direction would be needed that can successively be collected by the sonic anemometer over a long time period. This method provides similar results as the continuous planar fit method suggested by Ross and Grant (2015) by transforming the raw wind components into a coordinate system aligned with the long-term mean wind vector for each wind direction. However, this is likely to push the computational capacities of a CR1000 datalogger to its limits. In future versions of the REA system, this coordinate transformation may be implemented.

Again, since post-processing is not available for REA systems, effects of these differences and the impact of the filter time constant cannot be easily determined. They may be simulated by using high-frequency data collected by an EC system, which goes beyond the scope of this study.

4.3. Technical aspects

An engineering challenge with this kind of REA system is to maintain the pressure differences between the boxes and the atmosphere. Pelican boxes with a wide lid are preferable from a maintenance point of view, since they allow easy access to the internal reservoirs and components. On the other hand, they are not originally designed for large pressure differences, and the gasket along the edge of the lid tends to leak. During under-pressure in the box this is less critical, because atmospheric pressure presses the lid onto the gasket. But during periods of over-pressure, leaking air often makes the air pump work in short intervals to keep the pressure, even when no air is taken from the reservoirs. The seals had to be reinforced to avoid pressure drops that prevented the Tedlar bags from being completely emptied.

Another potential weakness is the durability of the Tedlar bags. The frequent filling and emptying stresses the material in a way that small punctures may appear after some weeks of operation. The effect of these leaks is not readily visible in the flux data, but in the raw gas

concentration data they appear in forms of distinct trends instead of the anticipated constant concentration during reservoir analysis (cf Fig. 5). For enhanced durability we replaced the Tedlar bags by multilayer gas sampling bags (Teknolab Sorbent, Kungsbacka, Sweden) with promising results. During the first two months of operation, no bag had to be replaced.

4.4. Comparison with other REA systems

The REA system introduced here has several advantages over previously described models. Besides the gas analyser, which is replaceable by virtually any other gas analyser, the sampling system is running on 12 V DC and is designed in a rugged, portable, and modular way. This makes it suitable for remote measurement campaigns with no grid power and little to no infrastructure, especially when using battery driven gas analysers. Furthermore, the replaceable analyser opens the opportunity to measure fluxes of any non-sticky gas species including isotopic tracers. For even more versatility one can install several gas analysers in a sequence. Since the “ballonet” principle is used for filling the reservoirs instead of the common approach to install a pump prior to the reservoirs, our system prevents potential contamination during sampling by avoiding any direct contact with pumps. This was implemented similarly by Haapanala et al. (2006), but since our sample air was analysed on site, the system described here used the same principle also for emptying the reservoirs and directing the air towards the analyser.

In common with the system described in Hornsby et al. (2009) and Haapanala et al. (2006) our system uses separate sample lines, which reduces the risk of mixing updraft and downdraft air during low dead-band velocity limits. Only few studies so far have calculated or discussed the limit of detection for the REA system by taking into account the variability of σ_w (e.g., Hornsby et al., 2009; Sarkar et al., 2020). Here we proposed a simple method based on Monte Carlo simulations and the analyser’s precision to calculate the system’s detection limits in relation to σ_w . This detection limit can easily be implemented in the downstream data processing workflows.

4.5. Concluding remarks

The presented REA system has worked reliably during several months in the Nordic climate, both during hot summer days and harsh winter conditions, covering ambient temperatures between -20°C and $+30^\circ\text{C}$. Measured fluxes of CO_2 and H_2O agree well with fluxes measured independently by the EC technique. In particular the good agreement of the H_2O fluxes indicates that no condensation takes place inside the tubes or reservoirs. The similarity in the technology and the determined detection limits make us confident that the REA system even captures fluxes of CH_4 and N_2O well.

The “ballonet” principle for filling and emptying the reservoirs is a reliable technology that provides constant flow rates without contamination by air pumps. Leakage of the pressure containers, however, is a certain problem that causes unnecessary pump action, but normally doesn’t hamper the system’s performance whatsoever.

The possibility to use slow response gas analysers makes the system relatively inexpensive for common greenhouse gases, and the time-sharing operation offers possibilities for parallel measurements of, e.g., soil fluxes, vertical concentration gradients, or fluxes by the profile method (Brutsaert, 1982). Here, the system was successfully used for chamber measurements during idle periods of the gas analyser. Shorter periods for analysis of REA reservoir concentrations would further expand this potential.

The G2508 analyser used in this study even provides NH_3 concentrations. However, the tendency of NH_3 to adsorb to tubing (Shah et al., 2006) and other challenges in measuring NH_3 fluxes reliably (Nelson et al., 2017) may limit the REA system’s applicability here and need yet to be studied.

Still, the possibility to chain different gas analysers in the air flow during reservoir analysis makes the system capable to measure fluxes of a virtually unlimited number of non-adsorbing gas species simultaneously.

In conclusion, this system provides new, affordable means to measure all relevant greenhouse gas fluxes at an ecosystem scale, which has not been feasible before.

4.6. Further development

In an updated version of our REA system we replaced the CR1000 datalogger by a CR1000X datalogger and the SDM-CD16AC relay driver by an SDM-CD16S Solid-State DC Controller (Campbell Scientific, Logan, UT, USA), the A0702 pump by an A2000 pump (Picarro inc., Santa Clara, CA, USA), and the three-way solenoid valves by bistable valves (Buerkert, Ingelfingen, Germany). Furthermore, the seals of the pressure containers were reinforced by steel bolts through the rim. This way, power consumption and deterioration of components was reduced.

Declaration of Competing Interest

The authors declare that they have no known competing financial interests or personal relationships that could have appeared to influence the work reported in this paper.

Acknowledgements

We greatly acknowledge Sören Hedwall for providing access to the field site and Bengt Norén for valuable engineering advice. This study was funded by the Swedish foundation for agricultural research (Stiftelsen Lantbruksforskning) under contract no. O-18-23-169 SLF and the Faculty of Natural Resources and Agricultural Sciences at the Swedish University of Agricultural Sciences (SLU, ua 2015. 1.1.1-3295).

References

- Ammann, C., Meixner, F.X., 2002. Stability dependence of the relaxed eddy accumulation coefficient for various scalar quantities. *J. Geophys. Res.* 107, 10.1029/2001JD000649.
- Aubinet, M., Grelle, A., Ibrom, A., Rannik, Ü., Moncrieff, J., Foken, T., Kowalski, A.S., Martin, P.H., Berbigier, P., Bernhofer, C., Clement, R., Elbers, J., Granier, A., Grünwald, T., Morgenstern, K., Pilegaard, K., Rebmann, C., Snijders, W., Valentini, R., Vesala, T., 2000. Estimates of the annual net carbon and water exchange of forests: the EUROFLUX methodology. *Adv. Ecol. Res.* 30, 113–175.
- Beverland, J.J., Ónéill, D.H., Scott, S.L., Moncrieff, J.B., 1996. Design, construction and operation of flux measurement systems using the conditional sampling technique. *Atmos. Environ.* 30, 3209–3220. [https://doi.org/10.1016/1352-2310\(96\)00010-6](https://doi.org/10.1016/1352-2310(96)00010-6).
- Bowling, D.R., Turnipseed, A.A., Delany, A.C., Baldocchi, D.D., Greenberg, J.P., Monson, R.K., 1998. The use of relaxed eddy accumulation to measure biosphere-atmosphere exchange of isoprene and other biological trace gases. *Oecologia* 116, 306–315.
- Bowling, D.R., Delany, A.C., Turnipseed, A.A., Baldocchi, D.D., Mortsom, R.K., 1999. Modification of the relaxed eddy accumulation technique to maximize measured scalar mixing ratio differences in updrafts and downdrafts. *J. Geophys. Res.* 104, 9121–9133.
- Brutsaert, W.H., 1982. Evaporation into the Atmosphere 229.
- Businger, J.A., Oncley, S.P., 1990. Flux Measurement with conditional sampling. *J. Atmospheric Ocean. Technol.* 7, 349–352. [https://doi.org/10.1175/1520-0426\(1990\)007<0349:FMWCS>2.0.CO;2](https://doi.org/10.1175/1520-0426(1990)007<0349:FMWCS>2.0.CO;2).
- Desjardins, R.L., 1972. A Study of Carbon Dioxide and Sensible Heat Fluxes Using the Eddy Correlation Technique. Cornell University, pp. 119–175. Ph.D. dissertation.
- Desjardins, R.L., Pattey, E., Smith, W.N., Worth, D., Grant, B., Srinivasan, R., MacPherson, J.L., Mauder, M., 2010. Multiscale estimates of N_2O emissions from agricultural lands. *Agric. For. Meteorol.* 150, 817–824. <https://doi.org/10.1016/j.agrformet.2009.09.001>.
- Eugster, W., Merbold, L., 2015. Eddy covariance for quantifying trace gas fluxes from soils. *SOIL* 1, 187–205. <https://doi.org/10.5194/soil-1-187-2015>.
- Gaman, A., Rannik, Ü., Aalto, P., Pohja, T., Siivola, E., Kulmala, M., Vesala, T., 2004. Relaxed eddy accumulation system for size-resolved aerosol particle flux measurements. *J. Atmospheric Ocean. Technol.* 21, 933–943. [https://doi.org/10.1175/1520-0426\(2004\)021<0933:REASPS>2.0.CO;2](https://doi.org/10.1175/1520-0426(2004)021<0933:REASPS>2.0.CO;2).
- Grönholm, T., Haapanala, S., Launiainen, S., Rinne, J., Vesala, T., Rannik, Ü., 2008. The dependence of the b coefficient of REA system with dynamic deadband on atmospheric conditions. *Environ. Pollut.* 152, 597–603.

- Haapanala, S., Rinne, J., Pystynen, K.-H., Hellén, H., Hakola, H., Riutta, T., 2006. Measurements of hydrocarbon emissions from a boreal fen using the REA technique. *Biogeosciences* 3, 103–112. <https://doi.org/10.5194/bg-3-103-2006>.
- Hadden, D., Grelle, A., 2017. The impact of cultivation on CO₂ and CH₄ fluxes over organic soils in Sweden. *Agric. For. Meteorol.* 243, 1–8.
- Hargreaves, K.J., Wienhold, F.G., Klemetsson, L., Arah, J.R.M., Beverland, I.J., Fowler, D., Galle, B., Griffith, D.W.T., Skiba, U., Smith, K.A., Welling, M., Harris, G. W., 1996. Measurement of nitrous oxide emission from agricultural land using micrometeorological methods. *Atmos. Environ.* 30, 1563–1571. [https://doi.org/10.1016/1352-2310\(95\)00468-8](https://doi.org/10.1016/1352-2310(95)00468-8).
- Hornsby, K.E., Flynn, M.J., Dorsey, J.R., Gallagher, M.W., Chance, R., Jones, C.E., Carpenter, L.J., 2009. A relaxed eddy accumulation (REA)-GC/MS system for the determination of halocarbon fluxes. *Atmos. Meas. Tech.* 2, 437–448. <https://doi.org/10.5194/amt-2-437-2009>.
- Katul, G.G., Poggi, D., Cava, D., Finningan, J., 2006. The relative importance of ejections and sweeps to momentum transfer in the atmospheric boundary layer. *Boundary-Layer Meteorol.* 120, 367–375.
- Nelson, A.J., Koloutsou-Vakakis, S., Rood, M.J., Myles, L., Lehmann, C., Bernacchi, C., Balasubramanian, S., Joo, E., Heuer, M., Vieira-Filho, M., Lin, J., 2017. Season-long ammonia flux measurements above fertilized corn in central Illinois, USA, using relaxed eddy accumulation. *Agric. Forest Meteorol.* 239, 202–212.
- Osterwalder, S., Fritsche, J., Alewell, C., Schmutz, M., Nilsson, M.B., Jocher, G., Sommar, J., Rinne, J., Bishop, K., 2016. A dual-inlet, single detector relaxed eddy accumulation system for long-term measurement of mercury flux. *Atmos. Meas. Tech.* 9, 509–524. <https://doi.org/10.5194/amt-9-509-2016>.
- Parkin, T.B., Venterea, R.T., Hargreaves, S.K., 2012. Calculating the detection limits of chamber-based soil greenhouse gas flux measurements. *J. Environ. Qual.* 41, 705.
- Pattey, E., Edwards, G.C., Desjardins, R.L., Pennock, D.J., Smith, W., Grant, B., MacPherson, J.L., 2007. Tools for quantifying N₂O emissions from agroecosystems. *Agric. For. Meteorol.* 142, 103–119. <https://doi.org/10.1016/j.agrformet.2006.05.013>.
- Ren, X., Sanders, J.E., Rajendran, A., Weber, R.J., Goldstein, A.H., Pusede, S.E., Browne, E.C., Min, K.-E., Cohen, R.C., 2011. A relaxed eddy accumulation system for measuring vertical fluxes of nitrous acid. *Atmos. Meas. Tech.* 4, 2093–2103. <https://doi.org/10.5194/amt-4-2093-2011>.
- Riederer, M., Hübner, J., Ruppert, J., Brand, W.A., Foken, T., 2014. Prerequisites for application of hyperbolic relaxed eddy accumulation on managed grasslands and alternative net ecosystem exchange flux partitioning. *Atmos. Meas. Tech.* 7, 4237–4250. <https://doi.org/10.5194/amt-7-4237-2014>.
- Ross, A., Grant, E., 2015. A new continuous planar fit method for calculating fluxes in complex, forested terrain: a new continuous planar fit method for calculating fluxes. *Atmos. Sci. Lett.* 16, 10.1002/asl.580.
- Sarkar, C., Turnipseed, A., Shertz, S., Karl, T., Potosnak, M., Bai, J., Serça, D., Bonal, D., Burban, B., Lopes, P.R.C., Vega, O., Guenther, A.B., 2020. A portable, low-cost relaxed eddy accumulation (REA) system for quantifying ecosystem-level fluxes of volatile organics. *Atmos. Environ.* 242, 117764 <https://doi.org/10.1016/j.atmosenv.2020.117764>.
- Shah, S.B., Grabow, G.L., Westerman, P.W., 2006. Ammonia adsorption in five types of flexible tubing materials. *Appl. Eng. Agric.* 22, 919–923.
- Tsai, J.-L., Tsuang, B.-J., Kuo, P.-H., Tu, C.-Y., Chen, C.-L., Hsueh, M.-T., Lee, C.-S., Yao, M.-H., Hsueh, M.-L., 2012. Evaluation of the relaxed eddy accumulation coefficient at various wetland ecosystems. *Atmos. Environ.* 60, 336–347.

ACTA UNIVERSITATIS AGRICULTURAE SUECIAE

DOCTORAL THESIS NO. 2024:5

This thesis examined impacts of management intensity on greenhouse gas (GHG) fluxes from agricultural peatland. Fluxes from a set-aside grassland and a cultivated cropland on peat were analysed. Furthermore, flux measurement equipment was developed and improved. The set-aside grassland showed higher carbon dioxide emissions than the cultivated cropland. Nitrous oxide and methane emissions had minor influence on the GHG balance of both sides. These findings indicate that current policies that favour setting-aside agricultural peatland to reduce GHG emissions are ineffective.

Hannes Keck received his graduate education at the Department of Ecology at SLU, Uppsala. He holds a MSc in Environmental Sciences from SLU, a MSc in Agriculture from University of Copenhagen, and a BSc in Agricultural Sciences from Justus Liebig University of Giessen.

Acta Universitatis Agriculturae Sueciae presents doctoral theses from the Swedish University of Agricultural Sciences (SLU).

SLU generates knowledge for the sustainable use of biological natural resources. Research, education, extension, as well as environmental monitoring and assessment are used to achieve this goal.

ISSN 1652-6880

ISBN (print version) 9978-91-8046-274-7

ISBN (electronic version) 978-91-8046-275-4